Dynamics of Flexible Coils in an Isorefractive Rod/Coil Composite Liquid. 2. Ternary Solutions

Adam S. Cantor† and R. Pecora*

Department of Chemistry, Stanford University, Stanford, California 94305-5080

Received May 3, 1994®

ABSTRACT: The dynamics of macromolecules in ternary solutions consisting of a probe polymer, a matrix polymer, and a solvent are studied using dynamic light scattering (DLS) with refractive index matching and, as supporting techniques, static light scattering and viscometry. The probe is linear polystyrene (PS) of molecular weight 390 000, which was always present in dilute amounts. The matrix polymer is poly(*n*-hexyl isocyanate) (PHIC) of varying molecular weight and polydispersity, whose concentration ranged from dilute to semidilute. The solvents used are either 1,1,2,2-tetrachloroethane (TCE) or toluene. PHIC is completely isorefractive in TCE at 75.0 °C. At lower temperatures and in toluene it is nearly isorefractive, removing the direct contribution of the PHIC to the light scattering spectrum. DLS measurements of PHIC in chloroform show that the PHIC behaves as a wormlike chain with a persistence length of ~20 nm. Results from previous studies of PS in binary solution are used for comparison to its behavior in the ternary solutions, which contained varying amounts of PHIC. Ternary solution studies were conducted over a range of temperature from 25 to 75 °C. The translational diffusion coefficient of the PS in ternary solution decreases with increasing concentration of PHIC, but the overall dimension of the PS remains essentially constant for all solution conditions. The decrease in PS diffusion coefficient is smaller than that predicted by reptation. Comparison of the different fractions of PHIC shows that the translational diffusion coefficient of PS is affected by the flexibility of the PHIC. The PS diffusion coefficient for all the PHIC fractions depends on the end-to-end distance of the PHIC. A fast relaxational mode (not present in dilute PS solutions) was seen in the DLS spectra for samples above a certain onset concentration of PHIC. The amplitude of this relaxation is always a small portion of the DLS spectrum, ranging from 0 to 5% of the total intensity. Using the contour length of the wormlike chain for the apparent rod length gives an onset concentration for the fast mode of $CL^3 \sim$ 10–15. The physical cause for this relaxation is unclear, although several possible explanations for it are discussed.

1. Introduction

There has been much interest in recent years in the dynamic behavior of polymers in semidilute solutions. In dilute solution, polymer dynamics depend primarily on polymer–solvent interactions and interactions between different segments on a single polymer chain. In the semidilute regime, the polymer concentration is high enough to cause significant excluded-volume interaction between different polymer molecules. Consequently, these and other polymer–polymer interactions (Coulombic, dipolar, van der Waals, etc.) must be considered along with the interactions present in dilute solution.

Semidilute polymer systems are important in a wide variety of practical applications, particularly in polymer processing. Highly concentrated or melt systems are often difficult to process because of their extremely high viscosity. Conversely, very dilute solutions are often of little use because they contain very little polymeric material. Semidilute solutions contain enough material to be practical but are still capable of being easily processed.

In this work an isorefractive ternary system was selected to examine semidilute solution behavior. This technique involves the study of the tracer diffusion of a polymer through a background of semidilute "invisible" polymers. Polystyrene was used as the tracer polymer. Studies of polystyrene in binary solution are presented in the preceding paper[1] (hereafter referred to as I). Previous work on probe–polymer background systems has typically used polystyrene (a flexible coil) as the tracer polymer and another flexible coil polymer as the background. Background polymers have included poly(vinyl methyl ether)[2–5] and poly(methyl methacrylate).[3,6,7] Similar studies have been done using spherical tracer particles with a variety of flexible background polymers.[8–10] Other work has been done in concentrated sphere systems and in concentrated mixtures of spheres and stiff chains.[11–16] Jamil et al. have recently studied a coil (polystyrene)/rod [poly(γ-stearyl α,L-glutamate)] system in a solvent (toluene) in which the rod aggregates into fibrils.[17] In this study, the background polymer is a semirigid rod [poly(*n*-hexyl isocyanate)].

Due to their extended nature in solution, rigid or semirigid polymer chains are expected to show semidilute behavior at lower concentrations than flexible polymers. The theory of Doi and Edwards (DE)[18,19] has greatly influenced the development of the field of rodlike polymer dynamics. The DE theory describes the translation and rotation of stiff, uncharged linear polymers in nondilute solutions, by modeling them as infinitely thin and totally rigid rods. The only intermolecular force between the rods is that restricting them from passing through each other. The DE theory predicts a change in the length dependence of the rotational diffusion coefficient, Θ, from $\Theta \sim 1/L^3$ in dilute solution to $\Theta \sim 1/L^9$ in semidilute solution. Because of this large predicted change, the focus of semidilute studies of semirigid polymers has been on the rotational diffusion of rods in an entangling environment,[20–36] although it now appears that the translational diffusion may be a better indicator of semidilute behavior.[16,27,31] The influence of the structure and dynamics of semidilute rods on the translational motion of a dilute coil polymer has not yet been theoretically examined.

An important practical consideration for the choice of system here is that the semidilute polymer (PHIC) be isorefractive with the solvent. This removes its contribution to the light scattering spectrum (to first order, at least). It is also important to find a probe particle which

† Current address: 3M Masking and Packaging Systems Division, Building 230-1S-14, 3M Center, St. Paul, MN 55144.

® Abstract published in *Advance ACS Abstracts*, October 1, 1994.

0024-9297/94/2227-6817$04.50/0

is soluble in the background polymer/solvent system. Solubility can often be a difficult problem for stiff polymers, since an increase in polymer rigidity usually corresponds to a decrease in solubility. The most stiff polymers known are typically soluble as singlets only in very corrosive solvents, which makes them difficult to study.[37,38] Ternary phase studies have been done on systems similar to that used here, which indicate limited solubility for small amounts of polystyrene.[39,40]

The binary solution behavior of the polystyrene is presented in I. Experimental details are presented in section 2. The characterization of the PHIC in the two solvents using differential refractometry, SLS, DLS, and viscometry is presented in section 3. Sections 4 and 5 contain the experimental results for the ternary solutions, as well as interpretations of their dynamic behavior.

2. Experimental and Data Analysis

Light Scattering. The DLS and SLS systems have been described elsewhere,[16,41,42] and the data analysis methods have been described in I. The SLS system analysis used in I had to be modified for the ternary solutions studied here.

Each ternary solution had a polystyrene concentration of 1.00 (±.03) mg/mL at 20.0 °C. While construction of a Zimm plot requires a series of concentrations of polystyrene, the slopes of the lines in a Zimm plot corresponding to individual concentrations are generally quite similar as long as the concentrations are not too large. In the polystyrene/TCE binary solution the radius of gyration was determined using the individual concentrations (as described below), and those radii agreed within experimental error with those determined by extrapolating to zero concentration. Thus, the ternary solutions were analyzed as if the 1.0 mg/mL PS values were the zero concentration points determined in a Zimm plot.

Ordinarily, the molecular weight is taken as the value of 1/intercept from a Zimm plot. Here it was necessary to use the known value of the molecular weight, 390 000, because the intercepts taken from the different PHIC concentrations differ from each other and from the zero concentration intercept.

Two other concerns must be raised relating to this analysis. The first and more obvious is that at temperatures away from the isorefractive temperature of 75 °C the effect of scattering from the polyisocyanate must be considered. At 25 °C, the differential index of refraction of PHIC in TCE is 10 times smaller than that of polystyrene in TCE. The molecular weight of the PHIC also varies from 3 to 10 times less than that of the PS used. The amount of light scattered has a square dependence on dn/dc and is proportional to molecular weight (when one considers equal weights of polymer). Thus the amount of light scattered by equal weights of PHIC should be from 0.1 to 0.3% of that scattered by the polystyrene based on these considerations, which is below the capabilities of the experiment to detect.

Another, more subtle consideration is due to scattering from coupled concentration fluctuations of two different species. Thus, the angular dependence of the scattered light should depend on terms involving each form factor individually and on a term involving a product of the two form factors. The effect this will have on the calculated radius of gyration has been determined for an isorefractive ternary solution[43] following the theory of Benmouna et al.[44] The problem has been approached by considering that the measured values give an "apparent radius of gyration" which can then be related to the actual radius of gyration. The apparent radius of gyration is given as

$$R_{G;app}^{\ 2} = R_{G;a}^{\ 2}\left(1 + \frac{R_{G;b}^{\ 2} B}{R_{G;a}^{\ 2}(1 + 2A_{2,b}c_bM_b)}\right) \quad (1)$$

where the subscript a represents the visible component (PS) and b the invisible component (PHIC). B is defined as

$$B = b\frac{(4A_{2,a}A_{2,b}M_aM_bc_ac_b)}{(1 + 2A_{2,a}M_bc_b)} \quad (2a)$$

and

$$b = \frac{A_{2,ab}}{A_{2,a}A_{2,b}} \quad (2b)$$

where A_2 represents the respective thermodynamic second virial coefficients, M the molecular weights, and c the mass concentrations.

An estimate of the change in R_G from the above correction is on the order of 5% or less. Thus the R_G measured should be a good representation of the true R_G of the polystyrene in solution, especially given the uncertainties in measurement of ≈10%. The uncertainty in the values of R_G that are reported is relatively high, because the amount of information available to form a linear fit is less than that in a standard Zimm plot where a linear fit is constructed from points which were also determined by linear fits.

Differential Index of Refraction. The differential index of refraction (dn/dc) was measured as a function of temperature from 20 to 80 °C in 5 °C increments. The exception was from 70 to 80 °C where 2 °C increments were used. The experimental details are described in I. The optical matching point was determined by a linear fit of the dn/dc values as a function of temperature (Figure 1). These values were determined using a 10.0 mg/mL solution of the broad fraction of PHIC. The optical matching point at 488 nm was 74.9 ± 0.7 °C, and ternary solution experiments were performed at 75.0 °C. The optical matching point was 75.4 ± 0.7 °C at 436 nm and 74.3 ± 0.6 °C at 546 nm. No difference was seen in the dn/dc for the fractionated samples.

The index of refraction of toluene is close to that of PHIC but is never isorefractive. The differential index of refraction at T = 25.0 °C was 0.016 mL/g for λ = 488 nm and 0.015 mL/g for λ = 514 nm. This differential index of refraction decreases with increasing temperature and at 75.0 °C is similar to that of PHIC in tetrachloroethane at 25 °C (Figure 1). An extrapolation of these results indicates an isorefractive point at 105–115 °C. The boiling point of toluene, however, is 110.6 °C. Measurements in toluene were done at 514 nm, because a slight improvement in the index match was seen with increasing wavelength. This causes a decrease in scattered light intensity, however, by 23% compared with 488 nm due to the λ^{-4} dependence of intensity in Rayleigh scattering. A shift to 632.8 nm (He–Ne laser line) would be likely to improve the index match but would cause a drop in scattered intensity by a factor of 2.8, as well as severely limiting the maximum input power available.

Materials. The poly(*n*-hexyl isocyanate) (PHIC) used was synthesized and donated by Shaul Aharoni of Allied Corp. It was prepared[45] using a modification of Shashoua's[46] method. For poly(*n*-alkyl isocyanates) this involves an anionic polymerization of RN=C=O, where R represents the alkyl side chain in the resulting polymer. The PHIC was fractionated by Keep[29,30] using THF as a good solvent and water as a nonsolvent. Three samples were studied. The unfractionated sample prepared by Aharoni is referred to as sample A or "broad". The other two fractions (previously studied in cyclohexane[29,30]) were identified as "big" and "small". These will also be referred to below as fractions B and C, respectively. The 390 000 polystyrene was described in I.

FTIR Analysis. For the samples in tetrachloroethane, Fourier transform infrared (FTIR) spectra were obtained both before and after filtering to monitor any changes in concentration upon filtering. Approximately 0.4 mL of solution was collected for the FTIR measurements (enough to fill a demountable IR cell with a 0.5 mm spacer). These measurements were done on an IBM IR/98 (LWN = 15797.49) using a demountable liquid cell with IRTRAN-2 windows. All measurements were made with a DTGS detector using 2 cm^{-1} resolution. Teflon spacers of 0.1 and 0.5 mm were used, depending on sample concentration.

The concentration of PHIC was monitored at the 2860, 1690, 1470, 1340, and 1090 cm^{-1} lines. The polystyrene concentration was monitored at the 1605 cm^{-1} line. The peak comparisons were done using peak height. Since these were direct comparisons of samples, there was no need to determine a functional concentration dependence for each peak. All FTIR measurements were done under identical conditions to avoid differences in peak shape and height due to different spectrophotometer conditions (e.g., too fast a scan rate can lead to peak broadening). Since the measurements were single beam and referenced against air, several solvent reference lines (2550, 2520, 2480, 2425, 2380,

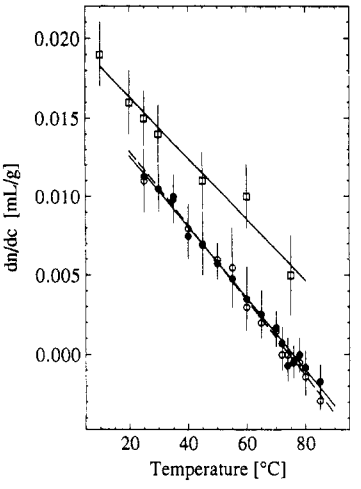

Figure 1. Differential refractive index of the broad fraction of PHIC as a function of temperature in the following solvents: (●) 1,1,2,2-tetrachloroethane, λ = 436 nm; (○) 1,1,2,2-tetrachloroethane, λ = 546 nm; (□) toluene, λ = 514 nm. The 514 nm data for toluene represent an interpolation of 436 and 546 nm results.

2070, and 1805 cm^{-1}) were monitored to ensure that the cell spacing was constant between measurements. The spacing of the interference fringes was also used as an independent check on the cell spacers.

The chief concern was that some of the polymer might be deposited on the filter, especially as the solutions become more concentrated and aggregation or poorly understood cooperative motions might be present. No change in either PHIC or PS concentration was seen for any of the samples. The samples in toluene were not monitored by FTIR because the toluene absorption bands obscure the peaks due to PHIC and PS. Ultraviolet (UV) spectroscopy could not be used, because both solvents absorb strongly in the UV region.

3. Binary Poly(*n*-hexyl isocyanate) Solutions

It is well-known that poly(*n*-alkyl isocyanates) are relatively stiff-chain molecules in solution.[47] The chain is an alternating carbon and nitrogen backbone which forms a helix with three twists for every eight monomers.

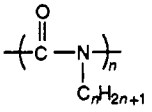

This helix arises because of steric interactions which prevent the chain from adopting a planar configuration. A twist along the backbone minimizes these interactions.

Two main possibilities have been proposed to explain the flexibility that is present in the chain. One is that reversals in the helix occur occasionally, causing a bend in the chain[48,49] Over a long enough contour length the chain would then appear similar to a flexible coil. The other idea is that small oscillations in the twist angle of the helix cause local flexibility in the chain. These oscillations would allow the chain to bend when observed over many bond lengths. This second reason is believed to be the primary cause of flexibility in chains with contour length similar to those used here.[50,51] Polar solvents increase this bond angle oscillation, thus increasing flexibility in comparison to nonpolar solvents. This increase in flexibility generally makes the polymer more soluble.

The PHIC was characterized in binary solutions in order to better understand the ternary solution dynamics (presented in sections 4 and 5). Because of the refractive index matching in tetrachloroethane and toluene, the PHIC could not be studied by light scattering in these solvents. However, the intrinsic viscosity was measured. DLS was performed on dilute solutions of PHIC in chloroform. The results from DLS and intrinsic viscosity can be used separately to calculate molecular shape and size parameters. A combination of these techniques provides more information than is possible using either one individually. The importance of determining the contour length of the PHIC is shown through a discussion of the Doi–Edwards theory for the semidilute regime. Finally, a comparison to previous experiments on PHIC in cyclohexane is presented. These previous experiments were done using the same fractions of PHIC, and it was thus expected that the results would agree closely with what was found here. It is seen, however, that the solvent has a significant effect on the PHIC.

DLS in Chloroform. Dilute solution samples in chloroform were analyzed using DLS with PHIC concentrations of 0.87, 0.17, and 0.50 mg/mL for fractions A–C, respectively. Scattering angles of 20°, 30°, and 55° were used. Lower angles were not included to avoid distortion of the distribution due to dust contributions, while at higher angles the sample scattering was too weak to accurately measure. DLS spectra were collected for as long as 15 h, yet they were much lower in quality than a typical polystyrene measurement. A signal-to-noise ratio for the correlation functions was determined in order to monitor the quality of the data. The second channel of the correlation function with the base line subtracted was used as the signal. The root mean square fluctuation in the delay channels was used as the noise. Signal-to-noise values of between 25 and 140 were obtained for individual correlation functions of PHIC in chloroform (compared to 1000–2000 obtained for polystyrene in tetrachloroethane).

The distribution of relaxation times was unimodal and relatively broad. At higher concentrations the DLS spectra of PHIC have been seen to become multimodal,[29,30] so concentrations in the dilute regime were used here. The distribution of diffusion coefficients was determined under the assumption that the PHIC was small enough so that rotational motion was not present in the DLS spectrum. The diffusion coefficients were 4.5 (±0.9) × 10^{-7}, 2.9 (±0.4) × 10^{-7}, and 4.9 (±0.7) × 10^{-7} cm^2/s for the broad, big, and small fractions, respectively. The broad fraction was measured at 20 °C, and the other two fractions were measured at 25 °C. Solvent values for the viscosity of chloroform were used for the subsequent calculations.

The diffusion coefficients were used to determine the lengths for a rodlike chain (Table 1). This was done using the corrected Broersma[52–55] theory (estimated to be valid for axial ratios greater than 5), which predicts

$$D = \frac{k_B T}{3\pi\eta_0 L}[\delta - \gamma] \tag{3}$$

where

$$\delta = \ln(2L/d) \tag{4a}$$

$$\gamma = -0.01713 + 4.154/\delta - 5.8/\delta^2 \tag{4b}$$

and d is the diameter of the chain. An estimate for the diameter of PHIC was taken as 1.4 nm.[29,30] Diameters of 1.5 and 1.6 nm have been reported elsewhere,[25,56–58] but changes in the diameter have a very small effect on the calculated length. The theory of Tirado and Garcia de la Torre[59,60] (T–G) could also be used for a rigid rod but only leads to small differences in the calculated length for axial ratios above 10 (as in this study).

The chain length can also be calculated using the Yamakawa and Fujii[61,62] (Y–F) theory for the translational

Table 1. Calculated Contour Lengths of PHIC Fractions (All Lengths in nm)

			Y–F (for given persistence length)				KAR (for given l_0)	
	Broersma	Tirado	infinite	30	25	20	0.17	0.20
big	128 ± 18	135 ± 18	140 ± 18	155 ± 24	160 ± 25	167 ± 27	105	96
small	64 ± 10	70 ± 11	74 ± 11	76 ± 11	78 ± 12	80 ± 12	59	53
broad	65 ± 12	70 ± 10	76 ± 10	77 ± 16	78 ± 16	80 ± 16	54	49

friction coefficient of a wormlike coil. The measured diffusion coefficient in the Y–F theory predicts the contour length of the chain for a given persistence length. For an experimentally determined diffusion coefficient, the predicted contour length decreases as the persistence length used in the calculation is increased. When $L < 2P$, the Y–F theory predicts essentially rigid-rod behavior. A discrepancy exists between the Y–F rigid-rod limit, T–G, and Broersma values for the diffusion coefficient of a rigid rod, due to the treatment of the ends of the rod ("end effects").

Intrinsic Viscosity. The intrinsic viscosity of a polymer solution may also be used to measure the size of the polymer. The intrinsic viscosity, $[\eta]$, is determined from the equation

$$\left(\frac{\eta}{\eta_0} - 1\right)\frac{1}{C} = [\eta] + k'[\eta]^2 C \tag{5}$$

where C is the mass concentration, η_0 the solvent viscosity, and k' the Huggins constant. Intrinsic viscosities for the PHIC were determined using ternary solutions. The value for a polystyrene 1.0 mg/mL solution was used for η_0 in the tetrachloroethane solutions. Similarly, the 2.0 mg/mL solution value was used for the toluene measurements. All intrinsic viscosities are for 25 °C. The intrinsic viscosities in tetrachloroethane were 74 ± 3, 247 ± 2, and 88 ± 3 mL/g for the broad, big, and small fractions, respectively. The intrinsic viscosity of the broad fraction was 126 ± 6 mL/g in toluene. These were determined using the low concentration solutions where the reduced specific viscosity was a linear function of concentration. k' was 0.49 ± 0.03, 0.80 ± 0.02, and 0.51 ± 0.17 for the three fractions in tetrachloroethane, respectively. These Huggins constants are consistent with those determined by Keep for the same fractions, with the largest fraction having the highest k' value. In toluene, k' was 0.75 ± 0.10. Others have found similar values for the Huggins constant, as well.[63] The intrinsic viscosities in tetrachloroethane are considerably lower than Keep's values. Although a decrease is expected as the polarity of the solvent increases, the change should not be so large. This is possibly due to aggregation in the nonpolar solvent as will be discussed further below.

An assumption about the shape of the polymer has to be made in order to determine its size using intrinsic viscosity. For a rigid rod, the Kirkwood–Auer–Riseman[47] (KAR) equation

$$[\eta] = \frac{4\pi N_A L^3}{90M \ln(2L/d)} \tag{6}$$

may be used to determine the intrinsic viscosity. The diameter, d, and the length per monomer, l_0, are required to determine the intrinsic viscosity for a given molecular weight. A diameter of 1.4 nm was used (see above), and the result was not highly dependent on this value since it only appears in the logarithmic term.

The length per monomer is more important, since it is needed to compare the length to the molecular weight. Values of l_0 between 0.11 and 0.24 nm have been reported in the literature.[47] The lower values of l_0 have been determined from dielectric measurements. X-ray diffraction, static light scattering, and molecular conformation calculations give l_0 in a range of 0.18–0.20 nm. Intrinsic viscosity studies have indicated l_0 to be about 0.17 nm.

The importance of the monomer length arises from the comparison of the viscosity results to the DLS results. The DLS results do not depend on the monomer length but only on the contour length of the polymer. The length of the chain calculated from the intrinsic viscosity depends on both the contour length and the molecular weight. The molecular weight can be simply related to the contour length if the monomer length is known. Thus a comparison of these two techniques requires that the monomer length be known.

The lowest values of l_0 that have been reported are not considered plausible, because they differ from the X-ray structure by so much. In general, previous studies have considered l_0 to be somewhere between 0.17 and 0.20 nm. Instead of selecting a particular value, the range of values from 0.17 to 0.20 nm is examined here.

It has been shown that the intrinsic viscosity of PHIC increases in solvents with decreasing polarity.[64] This is most likely due to the increasing stiffness of the polymer chain in these solvents. The intrinsic viscosity for a perfectly rigid rod should not be strongly affected by the solvent, since the intrinsic viscosity depends on the solvent only through the solvent's effect on the length and diameter of the rod. For a perfectly rigid rod it is not expected that the length would change with solvent. The diameter should not be affected enough to make a significant difference. Since the intrinsic viscosity is observed to decrease with increasing solvent polarity, this indicates that the chains are not entirely rigid, so that flexibility should be taken into account.

Yamakawa and Fujii[65] have developed a theory for the intrinsic viscosity of wormlike chains. As in their theory for translational diffusion, this theory consists of two cases: a chain more similar to a rigid rod, or a chain more similar to a flexible coil. The equations are not presented here due to their complexity but are essentially modifications of either the rigid or flexible limit. The two theories agree only for the rigid-rod limit where $d \to 0$ (or $L/d \to \infty$). The input parameters are the same as those for the KAR theory, with the persistence length as an additional parameter. A combination of the DLS and viscosity results can be used to estimate the persistence length.

Determination of Mark–Houwink Exponent. The relationship between the intrinsic viscosity and the molecular weight depends on the shape of the polymer. For a polydisperse system the intrinsic viscosity may be expressed as a power law dependence on molecular weight using the familiar Mark–Houwink equation

$$[\eta] = KM_v^a \tag{7}$$

where M_v is the viscosity-average molecular weight. For a non-free-draining random coil $a = 0.5$. For a free-draining coil $a = 1.0$ and $M_v = M_w$. For flexible chains the value of M_v generally lies between M_n and M_w.

The dependence of length is

$$[\eta] \propto L^2/\ln(2L/d) \tag{8}$$

using the KAR equation for a rodlike polymer. The value

of the exponent, a, in the Mark–Houwink equation can be determined from the slope of the plot of lot $[\eta]$ vs log [M]. For a rigid rod this value is not constant for all molecular weights. The slope for a particular molecular weight can be used to provide an "instantaneous" value for this exponent. This is determined by taking the derivative of log $[\eta]$ with respect to log [M]. For the KAR equation

$$a = 2.0 - 1/\ln(2L/d) \tag{9}$$

When the axial ratio approaches infinity, the value of the exponent a approaches 2. For axial ratios actually encountered experimentally (50–500), the exponent ranges from 1.75 to 1.85 for a rigid rod using the KAR equation. Using the Yamakawa–Fujii theory for a long, perfectly stiff wormlike coil, the value of a ranges from 1.70 to 1.80. The dependence of a on the persistence length and contour length for a wormlike coil has been calculated elsewhere.[42] A wormlike coil with P = 30 nm, L = 120 nm, and d = 1.4 nm has a = 1.2 using the Y–F formulas. For typical parameters ($20 < P < 40$, $20 < L < 200$, d = 1.4 nm) the value of a ranges from 1.15 to 1.40.

In the extremely long rod limit where a = 2, $M_v = (M_w M_z)^{1/2}$. For a relatively narrow fraction this would be approximately the average of M_w and M_z. As the value of a decreases toward 1, the value of M_v approaches more closely to M_w. For a wormlike coil $M_v > M_w$, but it is always closer to M_w that to M_z. The persistence length can be determined from the knowledge that M_v must lie between M_w and $(M_w M_z)^{1/2}$.

Polydispersity. In this study M_z (from DLS) and M_v (viscosity) were measured directly. The value of M_w was also necessary to find the persistence length, so it was determined by the breadth of the distribution measured by DLS. The uncertainty in M_w was large compared to M_z because the shape of the DLS relaxation time distribution was relatively large due to the weak scattering intensity of the PHIC solutions.

The distributions of chain lengths of the three fractions could be estimated from DLS using one of the three theories mentioned above (Broersma, Tirado and Garcia de la Torre, or Yamakawa and Fujii) which relate translational diffusion coefficients that are directly measured in DLS to molecular dimensions. This was done by suitably modifying the kernal of the CONTIN analysis program. The details of this procedure are given elsewhere.[42]

The polydispersity, M_z/M_w, was determined from the chain length distribution. Using the Broersma and T–G equations in the kernel of CONTIN gave nearly identical polydispersity values. Yamakawa and Fujii's results for large persistence lengths ($P > 50$ nm) agreed closely with the rigid-rod polydispersities. The polydispersity determined using Y–F with a persistence length of 20 nm was larger than the rod values by 30%.

Assuming a wormlike chain with P = 20 nm gave polydispersities of 1.89, 1.55, and 1.43 for the broad, small, and big fractions of PHIC, respectively. L_v was slightly larger than L_w, as expected. The relatively poor signal to noise of these measurements does not permit a precise calculation of the persistence length. The results were consistent with a wormlike chain with a persistence length between 20 and 40 nm, which is consistent with previous studies of PHIC in polar solvents.[56,58] Some of the individual fractions appeared to be consistent with one of the rigid-rod theories, but the results from all of the fractions could not be reconciled using either of the rod theories with a single value for the monomer length.

Semidilute Regime. An accurate determination of the length of the PHIC chains is important for characterizing the chain dynamics in the semidilute regime. Doi and Edwards[17–19] define the semidilute regime as

$$\frac{1}{L^3} \ll C \ll \frac{1}{L^2 d} \tag{10}$$

where L is the rod length, d the rod diameter, and C the number concentration. Semidilute behavior is not generally observed experimentally until CL^3 is 10–50.[23,30,66]

For a polydisperse system a sum may be taken over all of the different lengths present in solution. An "effective" value of CL^3 may be defined by

$$\sum_{i=1}^{N} C_i L_i^3 \tag{11}$$

where C_i is the number concentration of rods with length L_i. This definition is, of course, not rigorous but provides a rough measure of semidiluteness.

The number concentration of rods, C_i, is not directly observed in these experiments, however, and its determination from the DLS distribution involves considerable uncertainty. It may be shown that the sum in eq 11 is equivalent to $C_m L_z L_w/\sigma$ where C_m is the mass concentration and σ is the mass per unit length of the rod. The value of C_m is known when the sample is prepared. The monomer weight is 127 g, and the length per monomer is taken as 1.7–2.0 Å. This gives a value of 63.5–74.7 g/Å for σ. L_z is determined by the DLS experiment, and L_w may be calculated with a small loss of accuracy from L_z.

PHIC in Cyclohexane. Measurements of the same fractions of polyisocyanates were made by Keep,[29,30] and molecular weights higher than those determined here were reported. A careful comparison, however, shows that the results of the two studies are not inconsistent. The major difference is the solvents used in the two studies. Keep used cyclohexane for both viscometry and DLS. Cyclohexane is a nonpolar solvent, and the polymer chains are expected to be stiffer than they would be in a polar solvent.

The molecular weights used by Keep were determined using the Kirkwood–Auer–Riseman equation to relate the intrinsic viscosity to the length of the polymer chain. The viscosity results have a relatively small error, and most of the uncertainty in the length and molecular weight comes from the value of the monomer length, l_0, used in the KAR equation. Thus for the big PHIC fraction the following values may be calculated:

l_0 (Å)	L (Å)	M
2.0	1610	102 000
1.7	1760	131 000

The dilute solution DLS results (included in Table 2) may also be used to determine a hydrodynamic radius that can then be compared to the contour length by making assumptions about the stiffness of the chain (e.g., rod, worm, coil). The dilute solution values naturally have the

Table 2. Dilute Solution Results of PHIC in Cyclohexane from Keep and Pecora (1988)

		hydrodyn radius (Å)	
	conc (mg/mL)	DISCRETE	CONTIN
big PHIC, wet	0.17	157 ± 2	143 ± 4%
big PHIC, dry	0.0604	187 ± 27	[a]
big PHIC, dry, 40 °C	0.0604	168 ± 43	[a]
small PHIC	0.35	76 ± 5	66 ± 10%
	0.64	87 ± 3	71 ± 8%

[a] The error in the correlation functions was too large to obtain a meaningful result for these fractions by CONTIN analysis.

highest error of all the measurements, because the scattering power of the polyisocyanates is extremely weak. Furthermore, the DLS results of Keep were done with a scattering angle of 90°, and total collection times were 1 h or less. A major difficulty at such a high scattering angle is the need to use small sample times (typically, 3 μs), which caused the spectra to have contributions from photomultiplier afterpulsing as high as 60% of the total spectrum. In two instances the error was over 100% in the CONTIN analysis, and no values are reported in Table 2 for these solutions.

The apparent hydrodynamic radii presented by Keep[29,30] correspond to smaller molecular weights than the viscosity data by as much as 25%. Keep mistakenly assumes the viscosity average to be a z-average (which is what DLS measures) and thus describes an agreement of the viscosity and DLS values. Actually, the viscosity molecular weight should be smaller than the z-average molecular weight. In addition, the values previously reported in the literature were analyzed using DISCRETE,[30] which fits the DLS spectrum as a sum of single-exponential decays. CONTIN (which allows for broad distributions of relaxation times) is more appropriate when the distributions are not monodisperse. The CONTIN analysis gave hydrodynamic radius values 10–20% lower than from the DISCRETE analysis, which worsens the agreement between the viscosity and DLS results.

The most accurate of the dilute solution results is the big PHIC "wet" solution. A CONTIN fit to this data shows R_H = 14.3 nm (±4%), instead of 15.7 nm by DISCRETE. This corresponds to a rigid rod of length 134 nm using Broersma or 141 nm using Tirado–Garcia de la Torre. This compares closely with the CONTIN results determined in chloroform in this work. It is to be expected that the rigid-rod length determined should be slightly larger in the less polar solvent, cyclohexane. If considered to be a wormlike coil with a persistence length of 40 nm, then the big PHIC in cyclohexane has the same contour length as that determined in this work in chloroform assuming a persistence length of 25 nm. The small PHIC results indicate a length of between 50 and 70 nm using Broersma. The value depends on whether DISCRETE or CONTIN is used to analyze the data, as well as which concentration is used. This range, however, agrees with the results determined in chloroform in this work.

The DLS results in cyclohexane indicate a smaller length than the length determined by viscosity, which would be consistent with a small amount of aggregation. This would cause the viscosity molecular weight to appear larger. The DLS results might not detect this aggregation, because extremely large aggregates will scatter strongly but will move much more slowly than single chains. This would cause a very slow relaxation, which would appear as "dust" (i.e., small amounts of large-sized impurities which can be difficult to entirely remove from light scattering samples). A further interesting note is the agreement with the wet solution. This might indicate the absence of aggregation in water-saturated cyclohexane, which might be acting as a more polar solvent than pure cyclohexane (although still less polar than chloroform).

One further piece of evidence is that measurements of poly(n-butyl isocyanate) (PBIC) were made in chloroform, because it visibly aggregated in cyclohexane. The PBIC in chloroform showed the expected result of $L_v < L_z$. The intrinsic viscosity result of PHIC in toluene was similar in nature to the cyclohexane results. Using the KAR equation gives a length of 66–72 nm depending on the value used for the monomer length. This is approximately the same as the rigid-rod values determined from DLS, even though the DLS value should be considerably higher for a polydisperse fraction. It seems quite reasonable that some aggregation also occurs in the toluene samples, since aggregation of PHIC has been observed in toluene by dielectric relaxation measurements.[67]

The value for the length of the PHIC used in later analysis of the semidilute ternary systems is important in calculating a dimensionless concentration. Because of the larger lengths assumed by Keep, his values of CL^3 are higher than those used here for equal mass concentrations. For a 1.0 mg/mL solution of PHIC, CL^3 is 6.53 and 24.5 for the small and big fractions, respectively, if the lengths determined by Keep are used. Here the PHIC is determined to be a wormlike chain; however, the length of an equivalent rod (from Table 1) can be used to calculate CL^3. Using the lengths measured here, for a 1.0 mg/mL solution, CL^3 is 2.5 and 10.9 for the small and big fractions, respectively. Thus for equal mass concentration, the values for CL^3 calculated by Keep are 2–3 times larger than those calculated here (using an equivalent rod length). Values of CL^3 were also determined here by taking L to be the contour length of the wormlike chain. In this case, CL^3 is 3.9 and 15.9 for the small and big fractions, respectively, for a 1.0 mg/mL solution. This leads to a difference of ~1.5 in the calculated value of CL^3. In comparing results between the two studies, one may approximately consider the CL^3 values calculated by Keep to be twice those determined here for solutions of equal mass concentration.

4. Translational Diffusion of PS in Ternary Solution

The ternary solutions are composed of the two previously studied polymers, PS and PHIC in either 1,1,2,2-tetrachloroethane or toluene. The polystyrene is always present at 1.0 mg/mL concentration in the tetrachloroethane solutions. In the toluene solutions the concentration of polystyrene is 2.0 mg/mL. As discussed in I, the PS overlap concentration is 24.0 mg/mL, so the concentration of polystyrene is always dilute. The PHIC concentrations were chosen to extend from the dilute regime into the semidilute regime for the rodlike polymers. The PHIC is either completely isorefractive or nearly isorefractive, so that the predominant contribution to the light scattering spectra comes from the polystyrene.

Diffusive Modes of Ternary Solution. The PS/PHIC mixtures were studied with DLS at q^2 values of 4.2 × 10^9–1.16 × 10^{11} cm^{-2}. Typically measurements were made at 10 or 20 different scattering angles, varying at either 5° to 10° increments, from 20° to 130°. The predominant feature of the correlation spectra was a single mode which accounted for 95–100% of the intensity. It always showed a linear dependence between the relaxation frequency Γ and q^2, which is indicative of a translational diffusion process (a representative fit is shown in Figure 2). The values for the diffusion coefficients were taken from the slope of the linear fit of Γ vs q^2 and are shown in Table 3. The toluene values are shown in Table 6d.

A representative correlation function for a binary PHIC solution is shown in comparison to a binary PS solution correlation function in Figure 4. The PHIC spectra show no evidence of correlation. Similar spectra were obtained over a wide range of scattering angles, sample delay times, and total correlation times. All of these spectra showed no correlated behavior. The sample spectrum in Figure 3 was taken at a temperature of 25.0 °C, where the PHIC is not completely isorefractive. The difference in index of refraction ("contrast") is apparently too small to observe correlation above the background of solvent and dust scattering. This does not imply that scattering does not

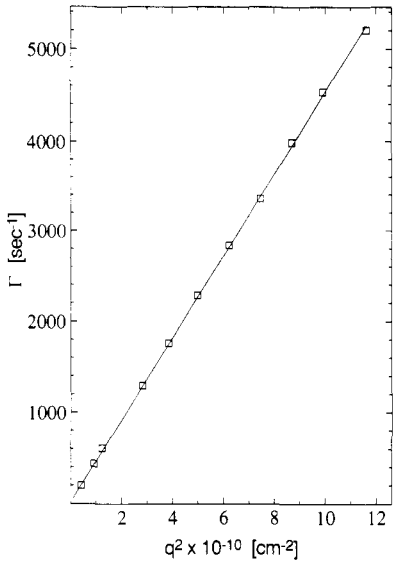

Figure 2. Relaxation constant, Γ, of the PS translational diffusion mode as a function of q^2. The sample was 1.0 mg/mL PS and 10.3 mg/mL broad PHIC in TCE at 25.0 °C. The slope of the linear fit represents the translational diffusion coefficient.

Table 3. Diffusion Coefficients [(cm^2/s) × 10^8] of Polystyrene in Ternary Solutions

conc (mg/mL)	25 °C	50 °C	75 °C
	a. Broad PHIC		
1.92	6.92 ± 0.03	12.03 ± 0.15	17.85 ± 0.10
4.04	6.46 ± 0.04	11.90 ± 0.11	17.34 ± 0.10
6.02	5.89 ± 0.05	10.96 ± 0.12	16.58 ± 0.22
10.08	4.47 ± 0.03	8.47 ± 0.15	13.43 ± 0.23
19.98	3.02 ± 0.02	6.63 ± 0.08	10.22 ± 0.14
29.96	2.09 ± 0.01	3.70 ± 0.07	6.48 ± 0.07
	b. Big PHIC		
0.36	7.69 ± 0.04	11.83 ± 0.08	18.06 ± 0.21
0.70	7.17 ± 0.07	11.45 ± 0.09	16.79 ± 0.06
1.14	6.86 ± 0.04	11.11 ± 0.08	17.10 ± 0.17
1.41	6.55 ± 0.04	10.25 ± 0.15	15.51 ± 0.17
2.00	5.92 ± 0.06	10.03 ± 0.06	17.65 ± 0.59
3.46	4.95 ± 0.14	7.90 ± 0.06	15.51 ± 0.04
6.00	4.41 ± 0.02	7.28 ± 0.07	11.59 ± 0.18
10.20	2.28 ± 0.04	3.43 ± 0.04	6.16 ± 0.15
	c. Small PHIC		
0.53	7.95 ± 0.09	12.45 ± 0.18	18.29 ± 0.14
1.28	7.41 ± 0.05	11.69 ± 0.07	17.42 ± 0.10
2.54	6.96 ± 0.12	11.23 ± 0.21	15.80 ± 0.29
3.12	6.78 ± 0.14	10.97 ± 0.28	15.77 ± 0.12
4.14	6.00 ± 0.05	9.70 ± 0.07	15.05 ± 0.51
8.38	4.62 ± 0.08	7.47 ± 0.05	13.14 ± 0.16
9.98	4.46 ± 0.11	6.88 ± 0.05	11.30 ± 0.11
15.02	3.27 ± 0.03		

occur where a slight index mismatch exists but only that it is too weak to detect in this way.

The diffusion coefficient of the PS decreased with increasing concentration of PHIC. At low concentrations of PHIC, the diffusion coefficient approached the dilute solution PS value. Thus, this mode corresponds to the translational diffusion of the polystyrene. It may be considered to be approximately the same as the self-diffusion coefficient of the PS. The DLS technique strictly measures mutual diffusion of macromolecules. As the polymer concentration is reduced to zero, this becomes equivalent to the self-diffusion coefficient. The use of the optical tracer technique here is of interest, because it is inferred that the tracer self-diffusion coefficient will be measured even as the matrix concentration increases. It has not been conclusively shown that a tracer experiment of this type will measure self-diffusion. However, comparisons of the results of optical tracer DLS and forced Rayleigh scattering (FRS) (which typically measures the self-diffusion coefficient) experiments on the same system

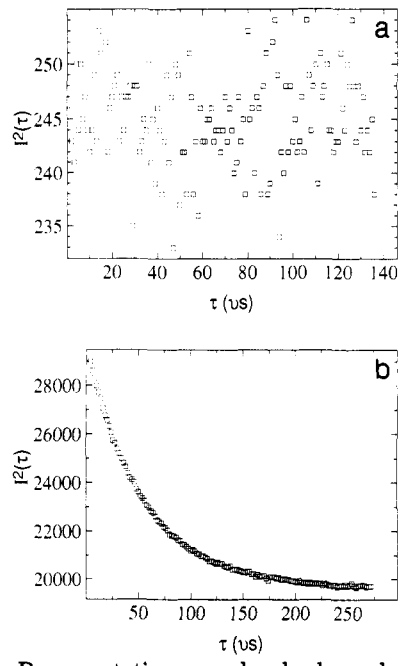

Figure 3. Representative second-order homodyne correlation functions, $G^{(2)}(\tau)$, taken at a temperature of 25.0 °C. a is for a 10.0 mg/mL PHIC in TCE solution at a scattering angle, θ, of 90.0°. b is for a 1.0 mg/mL PS in TCE solution at θ = 123.7°.

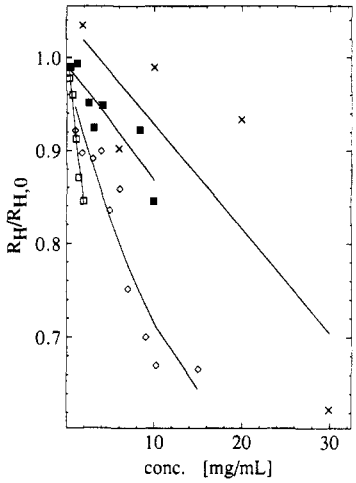

Figure 4. Y-axis representing the Stokes–Einstein hydrodynamic radius, R_H, of the polystyrene coil in ternary solution divided by R_H of the PS coil in the binary PS solution. This ratio is shown as a function of the mass concentration of PHIC in the ternary solution. At zero concentration this ratio is 1 by definition. The curves are drawn only to guide the eye. (×) Broad PHIC fraction in TCE. (□) Big PHIC fraction in TCE. (■) Small PHIC fraction in TCE. (◇) Broad PHIC fraction in toluene.

have shown the two diffusion coefficients to be the same (within an error of 10–15%).[68]

Static Light Scattering. The main purpose of the static light scattering is to look for changes in the solution behavior with changing amounts of PHIC. These measurements should be sensitive to aggregation, as this would increase the apparent radius of gyration. The radius of gyration values for the polystyrene in binary solution are shown in Table 4. The radius of gyration values for the polystyrene in ternary solution are shown in Table 5. Any difficulties with excess scattering at low scattering angles could be attributed either to dust in the samples or to stray light from cell interfaces. Neither problem was correlated with sample concentration, and this excess scattering was present in binary solutions and pure solvent as well.

Table 4. Radii of Gyration (nm) of Polystyrene in Binary Solution

PS conc (mg/mL)	25 °C	50 °C	75 °C
(Zimm)	31.0 ± 1.7	31.2 ± 1.4	30.2 ± 1.8
0.50	31.8 ± 2.3	31.9 ± 2.4	30.7 ± 2.3
1.00	33.0 ± 1.9	31.2 ± 2.1	31.9 ± 2.3
1.50	27.8 ± 2.2	31.7 ± 2.1	31.0 ± 3.3
2.00	31.0 ± 2.0	33.3 ± 2.4	30.7 ± 2.4
2.50	32.4 ± 1.9	31.4 ± 2.4	31.8 ± 3.5

Table 5. Radii of Gyration (nm) of Polystyrene in Ternary Solution

PHIC conc (mg/mL)	25 °C	50 °C	75 °C	avg
	a. Broad PHIC/PS/TCE			
1.92	32.7 ± 3.6		29.1 ± 3.7	30.9
4.04	31.1 ± 1.8		29.7 ± 4.1	30.4
6.02	31.6 ± 3.2		31.2 ± 3.8	31.4
10.08	31.5 ± 1.8		34.1 ± 2.3	32.8
19.98	34.0 ± 1.9		32.0 ± 3.0	33.0
29.96	31.2 ± 1.8		32.0 ± 3.0	31.6
	b. Big PHIC/PS/TCE			
0.36	31.9 ± 2.1	33.1 ± 2.1	32.4 ± 2.4	32.5
0.70	28.6 ± 2.3	33.7 ± 2.5	31.3 ± 2.4	31.2
0.70	31.8 ± 2.2	35.4 ± 3.1	33.5 ± 2.5	33.6
1.14	31.6 ± 2.6	33.7 ± 2.9	31.3 ± 2.7	32.2
2.00	24.1 ± 2.4	24.9 ± 2.7	22.6 ± 1.6	23.9
3.46	30.4 ± 2.2	31.4 ± 2.2	30.0 ± 2.0	30.6
6.00	27.6 ± 2.2	28.8 ± 2.2	27.6 ± 2.3	28.0
10.20	26.5 ± 1.9	26.7 ± 2.0	25.0 ± 2.1	26.1
	c. Small PHIC/PS/TCE			
0.53	32.1 ± 2.3	33.0 ± 2.7	32.0 ± 2.0	32.4
1.28	33.0 ± 2.4	31.6 ± 1.9	32.2 ± 2.4	32.3
2.54	31.8 ± 2.3	33.6 ± 2.5	31.9 ± 1.9	32.4
3.12	31.2 ± 2.2	33.0 ± 2.3	31.6 ± 2.0	31.9
4.14	31.0 ± 2.1	31.2 ± 2.0	30.0 ± 1.7	30.7
9.98	31.3 ± 2.0	31.3 ± 3.8	30.6 ± 4.1	31.1

The radius of gyration measured here was essentially constant over the entire PHIC concentration range. In the big PHIC there seemed to be a slight coil contraction, since R_G for the highest concentration sample was ~20% smaller than for the binary PS solution. A decrease in the radius of gyration of a tracer coil has been predicted and observed by many in both binary and ternary concentrated polymer solutions.[69] The deviation observed here would be consistent with these previous observations, but it should be noted that it was only marginally larger than the experimental error.

These results show that the size of the coil in solution may decrease slightly with increasing PHIC concentration but generally remains constant over the range of concentrations used here. There is also no indication of polystyrene aggregation with increasing concentrations of PHIC.

Stokes–Einstein Behavior. If one observes the macroscopic viscosity of the solutions, then a comparison to Stokes–Einstein behavior may be made. Essentially this consists of using the solution viscosity instead of the small-molecule solvent viscosity (here TCE or toluene) in the Stokes–Einstein equation

$$D = \frac{k_B T}{6\pi\eta R_H} \tag{12}$$

If R_H, the apparent hydrodynamic radius, remains constant with changing viscosity, then the solution is considered to show S–E behavior. This indicates that the particle motion is governed by the macroscopic composition of the solution, rather than by the local geometry. For all fractions, the effective hydrodynamic radius of the coil decreases with increasing concentration of PHIC (Table 6 and Figure 4). For comparison purposes the hydrodynamic radius of the

Table 6. Effective Hydrodynamic Radius and Translational Diffusion of Polystyrene, MW = 390 K, in Ternary Solution (Temp = 25 °C)

conc (mg/mL)	diff coeff × 10^8 (cm^2/s)	viscosity (cP)	effective hydrodyn radius (nm)
	a. Broad PHIC/TCE		
0.00	8.25	1.84	14.38
1.92	6.92 ± 0.03	2.12	14.88 ± 0.06
4.04	6.46 ± 0.04	2.48	13.64 ± 0.08
6.02	5.89 ± 0.05	2.85	12.99 ± 0.11
10.08	4.47 ± 0.03	3.43	14.24 ± 0.10
19.98	3.02 ± 0.02	5.38	13.43 ± 0.09
29.96	2.09 ± 0.01	11.64	8.97 ± 0.04
	b. Big PHIC/TCE		
0.00	8.25	1.84	14.38
0.36	7.69 ± 0.04	2.02	14.07 ± 0.07
0.70	7.17 ± 0.07	2.21	13.80 ± 0.13
1.14	6.86 ± 0.04	2.42	13.13 ± 0.08
1.41	6.55 ± 0.04	2.66	12.52 ± 0.08
2.00	5.92 ± 0.06	3.03	12.17 ± 0.12
3.46	4.95 ± 0.14		
6.00	4.41 ± 0.02		
10.20	2.28 ± 0.04		
	c. Small PHIC/TCE		
0.00	8.25	1.84	14.38
0.53	7.95 ± 0.09	1.93	14.23 ± 0.16
1.28	7.41 ± 0.05	2.06	14.30 ± 0.10
2.54	6.96 ± 0.12	2.29	13.70 ± 0.24
3.12	6.78 ± 0.14	2.42	13.30 ± 0.27
4.14	6.00 ± 0.05	2.67	13.64 ± 0.11
8.38	4.62 ± 0.08	3.56	13.27 ± 0.23
9.98	4.46 ± 0.11	4.02	12.17 ± 0.30
15.02	3.27 ± 0.03		
	d. Broad PHIC/Toluene		
0.00	2.65	0.67	12.24
1.02	2.41 ± 0.09	0.80	11.28
1.81	2.18 ± 0.08	0.91	10.99
3.01	1.93 ± 0.04	1.04	10.92
3.97	1.77 ± 0.08	1.12	11.01
5.01	1.58 ± 0.09	1.35	10.23
6.03	1.36 ± 0.10	1.53	10.52
7.02	1.38 ± 0.03	1.72	9.20
9.02	1.17 ± 0.04	2.18	8.58
10.20	1.04 ± 0.02	2.56	8.21
14.99	0.67 ± 0.03	3.98	8.17

polystyrene in binary solution was determined using the 1.0 mg/mL PS in TCE (or 2.0 mg/mL PS in toluene) viscosity and diffusion coefficient. This gives a slightly smaller value than the dilute solution hydrodynamic radius which uses the solvent viscosity and the zero concentration diffusion coefficient.

For low concentrations the hydrodynamic radius remains unchanged. As the concentration increases the hydrodynamic radius decreases by up to 15% in most instances. In one case (30 mg/mL broad PHIC) R_H decreases by 35%. The decrease in R_H indicates that the chain is not being slowed down as strongly as the S–E equation predicts on the basis of the macroscopic solution viscosity.

Deviations from S–E behavior have been seen in a wide variety of experimental systems,[8,10,11,70–72] and several explanations for the deviations have been presented. Most of these studies have examined spherical probes, but simple S–E diffusion of a random coil has been shown to be the same as that of a hard sphere.[70] It has been suggested that a random coil will shrink in size as the matrix concentration increases,[73] but the static light scattering measurements indicate that the radius of gyration does not significantly change.

It is possible that deviations from S–E behavior could be due to local topology. If the distance between entanglements (or "mesh size") of the rodlike polymer is larger than the probe size, the probe may be able to move

through the solution without having to displace the entangling polymers. The probe could therefore move faster than indicated by the macroscopic solution viscosity, which would lead to a smaller measured hydrodynamic radius. Under this assumption, an increase in the deviation from S–E behavior would occur with increasing matrix size and decreasing probe size. Solutions of this type have been denoted as "underconstrained".[11] The most obvious example of this type of motion occurs in a gel where the overall solution does not flow (i.e., infinite viscosity), yet small probes inside the gel continue to diffuse.

The strongest deviation (by mass concentration) from S–E behavior seen in this study was for the big fraction of PHIC. This would be consistent with the explanation given above, although even for this fraction the average contour length (~160 nm) of the matrix polymer is only 5 times greater than the average size (give by R_G) of the probe. The broad fraction in toluene showed a mildly stronger deviation than it did in TCE. This might be consistent with the increased stiffness of the PHIC in toluene, since it would be more extended (and thus behave as if it were a larger molecular weight). The average contour length of the smaller PHIC fraction, however, is only about twice as large as the probe. It seems unlikely that the characteristic mesh size could be large enough to allow the probe to move between entangling points without encountering their resistance.

Another explanation for S–E deviations centers around cooperative motions of the probe and matrix. It has been postulated that interactions between the probe and matrix can perturb the translational diffusion of the probe.[8,10,70] Where the matrix translates faster than the probe, it is expected to increase the translational diffusion of the probe. This effect should depend primarily on the amount of matrix polymer present and not as strongly on matrix size. This seems to provide a more reasonable explanation for the deviations seen in the low molecular weight samples. It does not explain why the higher molecular weight sample shows stronger deviations on a per mass basis. It is possible that both effects described above (underconstraint, cooperative motion) could be affecting the high molecular weight matrix solutions. It should be noted, though, that the deviations are not extremely large, so the solution may be loosely considered to show S–E diffusion.

Stretched Exponential Calculations. A number of different ways are available to characterize the dependence of the diffusion coefficient of the PS on the concentration of PHIC. The well-known reptation theory leads to a power law dependence, $D_{PS} \propto [c_{PHIC}]^{-\nu}$. If a power law dependence holds for the entire range of concentrations, then the log(D) vs log(c) plot would be a straight line with a slope of $-\nu$. However, there is no particular value of ν which will characterize the diffusion coefficient over the entire range of concentrations studied. Rather, it is instructive to consider the slope of a tangent drawn to the curve of a log(D) vs log(c) plot. This can be considered to show the concentration dependence at a particular concentration.

It is difficult to graphically select a tangent to the log(D) vs log(c) plot due to the error in the data. A consistent way to find this value is to fit the experimental data to a stretched exponential concentration dependence

$$D = D_0 \exp(-\alpha c^u) \tag{13}$$

This function has been shown to adequately represent the concentration dependence in several studies, although the existence of an underlying physical basis for this is still uncertain.

Table 7. Translational Diffusion Coefficient of PS in Ternary Solutions: Stretched Exponential Fits with Fixed D_0

temp (°C)	α (mg/mL)	u
	Big	
25	0.178 ± 0.018	0.81 ± 0.06
50	0.162 ± 0.022	0.85 ± 0.08
75	0.080 ± 0.018	1.10 ± 0.19
	Small	
25	0.081 ± 0.005	0.90 ± 0.04
50	0.076 ± 0.011	0.89 ± 0.07
75	0.071 ± 0.006	0.88 ± 0.04
	Broad	
25	0.088 ± 0.006	0.81 ± 0.04
50	0.027 ± 0.003	1.12 ± 0.11
75	0.020 ± 0.002	1.18 ± 0.08
	Broad, Toluene	
25	0.112 ± 0.006	0.88 ± 0.04

Table 8. Translational Diffusion Coefficient of PS in Ternary Solutions: Stretched Exponential Fits with Floating D_0

temp (°C)	$D_0 \times 10^8$ (cm²/s)	α (mg/mL)	u
		Big	
25	8.12	0.159 ± 0.025	0.86 ± 0.16
50	12.11	0.094 ± 0.015	1.09 ± 0.23
75	17.20	0.015 ± 0.002	1.85 ± 0.37
		Small	
25	8.29	0.081 ± 0.008	0.90 ± 0.09
50	12.72	0.052 ± 0.006	1.09 ± 0.10
75	19.12	0.081 ± 0.015	0.83 ± 0.10
		Broad	
25	7.94	0.067 ± 0.006	0.89 ± 0.15
50	12.91	0.069 ± 0.011	0.87 ± 0.22
75	18.83	0.036 ± 0.004	1.02 ± 0.17
		Broad, Toluene	
25	27.80	0.143 ± 0.009	0.85 ± 0.10

Fits to the data were determined using the measured values of D_0 (Table 7) and also by allowing D_0 to be a floating parameter (Table 8). The fixed D_0 fits are shown in Figure 5. In this case, D_0 is the diffusion coefficient for zero concentration of PHIC. Since all solutions in TCE had 1.0 mg/mL PS, the value for D_0 was taken from the 1.0 mg/mL binary solution of PS in TCE. The values used for D_0 were 8.25, 13.06, and 18.91 × 10^{-8} cm²/s for the respective temperatures of 25, 50, and 75 °C. These were determined from a linear fit to the diffusion coefficient vs PS concentration at each temperature rather than using the individual measured value for PS concentration of 1.0 mg/mL at each temperature. The values of the exponent u were between 0.8 and 1.2. A tangent at any particular concentration could be found from the stretched exponential fit. The slope at a particular concentration is $-auc^u$. This slope can be taken as an effective value of the exponent ν for a simple power law dependence. The values of ν determined in this way varied from 0.05 to 1.6 over the entire concentration range studied.

Comparison to Reptation. The reptation theory may be used to predict the dependence of the self-diffusion coefficient of a flexible chain as a function of molecular weight and concentration. The original theory of reptation[74] describes the motion of a flexible chain molecule amidst a network of fixed obstacles. This has since been extended to include systems where the obstacles, although not fixed, remain stationary long enough to behave as fixed obstacles. In the common case where the obstacles are also flexible chains, de Gennes has shown using scaling arguments that $D \propto c^{-1.75}$ in a good solvent and $D \propto c^{-3.0}$ in a θ solvent.[73] It is natural to expect that where the entangling network consists of semirigid polymers any shift

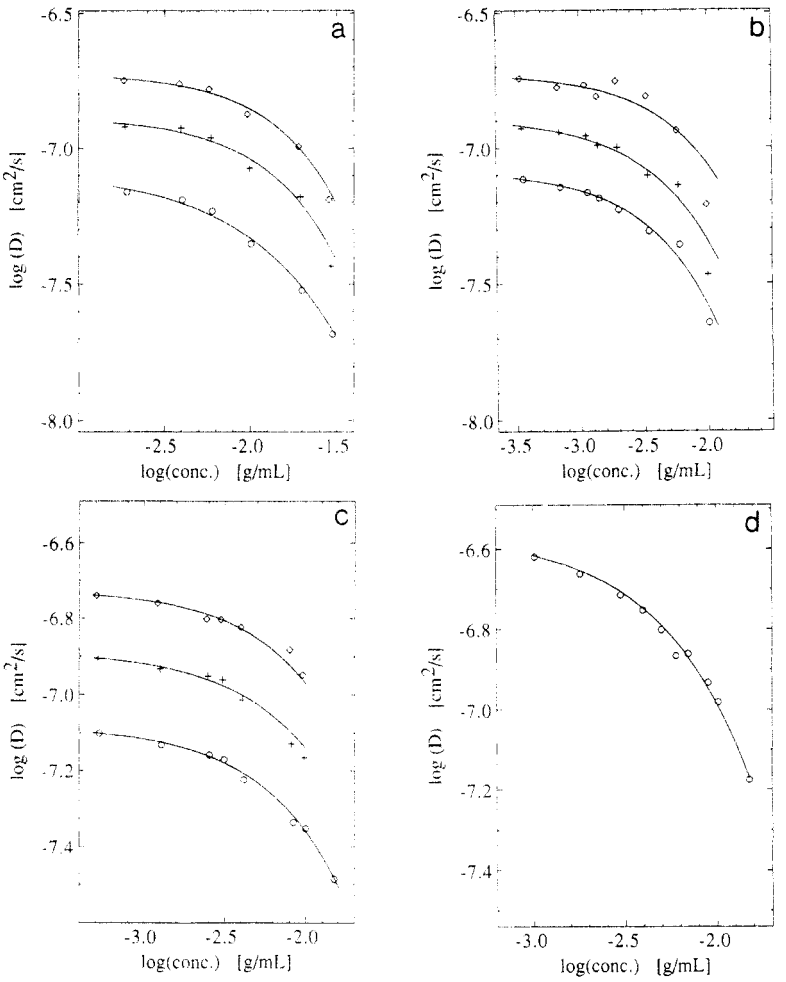

Figure 5. Translational diffusion coefficient of the polystyrene coil in the ternary solution as a function of temperature and the concentration of PHIC. The curves represent stretched exponential fits to the data using a fixed value for D_0. a–c are for the broad, big, and small fractions, respectively, in TCE. d is for the broad fraction in toluene. (○) Temperature = 25.0 °C. (+) Temperature = 50.0 °C. (◇) Temperature = 75.0 °C.

in concentration dependence should be toward more negative exponents. This would stem from the more extended nature of a semirigid polymer in comparison to a flexible chain polymer, which should cause stronger entanglement at lower concentration. For sufficiently high overlaps of polymer the overall nature of the chain should become less important.

Comparison to the experimental results obtained here for the PS in PHIC, however, shows that in no case does the concentration dependence reach that predicted by de Gennes' version of reptation. These concentrations are certainly high enough to ensure that the rods are in close proximity to each other. Two possibilities exist to explain the absence of reptation. One is the idea of an underconstrained solution, but as described above in the discussion of Stokes–Einstein results this is unlikely.

The second, and more likely, possibility is for the relaxation of the network to be faster than the reptation time of an individual chain. More simply stated, the blocking rods will more away from the coil more quickly than the coil can reptate. When this happens the coil can move as a whole into the region vacated by these rods. It is probably more accurate to consider this as a cooperative motion of coil and network, so that the coil in essence moves through the solution as a unit "pushing" the blocking rods out of the way. The network will relax before the coil can ever reptate a significant distance. This will allow movement of the whole coil, which is a much more likely mode of transport for a coil undergoing random motion.

Hydrodynamic Scaling Theory. Phillies' hydrodynamic scaling model predicts a stretched exponential form (see eq 13) for the concentration dependence of D. This functional form has been observed to agree with a number of experimental studies. The hydrodynamic scaling model also predicts values of α and u for given molecular weights of matrix and probe. In the limit of low matrix molecular weight ($M_m < 50\,000$) $u = 1.0$, and at high M_m ($M_m > 500\,000$) $u = 0.5$. In between these two values is a crossover region where u is between 0.5 and 1.0. The experimental data analyzed by Phillies indicates $u \sim M_m^{-1/4}$ in this crossover region. Wheeler and Lodge see qualitative agreement for polystyrene in a PVME background (140 000 M_m PVME has u of 0.63–0.70). In this study the PHIC molecular weights are in the 50 000–100 000 range and the values of u measured range from 0.8 to 1.2. There is also a slight tendency toward a decreasing u with increasing matrix molecular weight, which agrees with the hydrodynamic scaling model.

The values of α measured here are of the same order of magnitude as those predicted by Phillies. The temperature dependence of these values is difficult to understand. The small PHIC fraction gives results independent of temperature. The results for the big fraction do not change for 25 and 50 °C but show a decrease in α and an increase in u for 75 °C. The broad fraction results are similar at 50 and 75 °C but change at 25 °C. It is possible that this is due to the imprecision in the fitting process (at least insofar as these differences appear to be discrete changes instead of smooth dependences on temperature). That

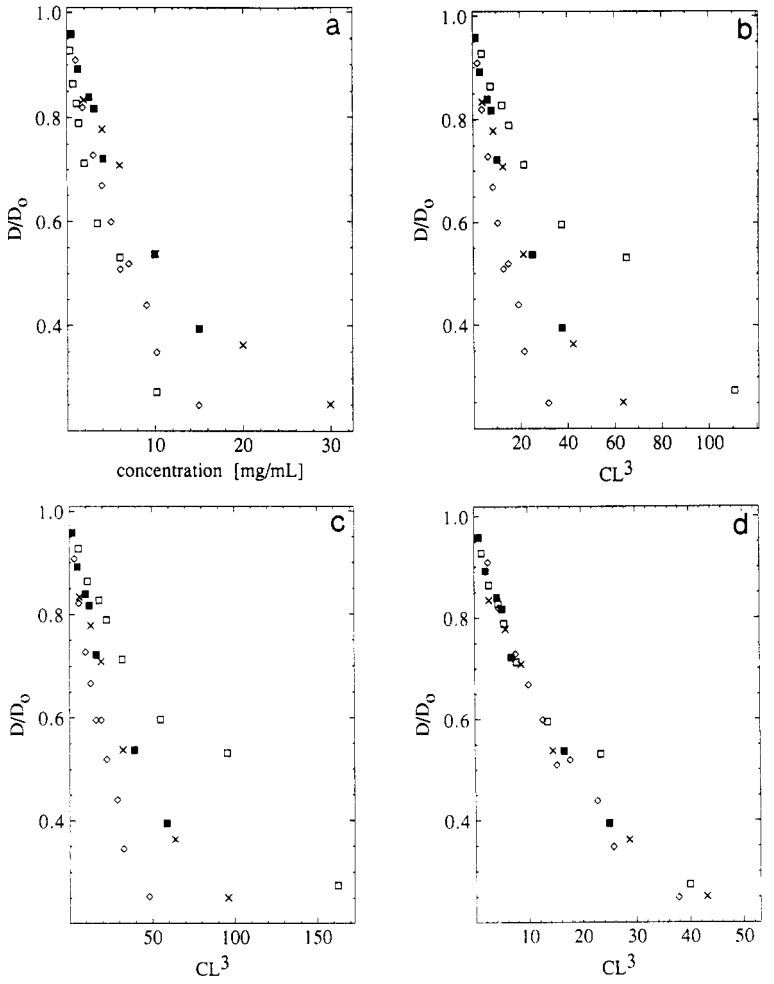

Figure 6. Reduced translational diffusion coefficient, D/D_0, of the polystyrene coil as a function of concentration of PHIC in the ternary solution. a is for mass concentration. b is for a reduced concentration, CL^3, where L is taken from Broersma's equation. c is for CL^3 where L is the contour length of a wormlike chain from Yamakawa and Fujii. d is for CL^3 (or $CL\langle R^2\rangle$) where L is replaced with the end-to-end distance of the wormlike chain. All of the plots are for T = 25.0 °C. (×) Broad PHIC fraction in TCE. (□) Big PHIC fraction in TCE. (■) Small PHIC fraction in TCE. (◇) Broad PHIC fraction in toluene.

these values change, however, seems to indicate an effect which might not be predicted by hydrodynamic scaling.

The value of α depends on several parameters: $R_{G,a}$, $R_{G,m}{}^3$, a_0, and M_m. $R_{G,a}$ is the radius of gyration of the probe, and this is seen to be essentially constant with temperature. M_m and a_0 should not be affected by temperature. $R_{G,m}$ is the radius of gyration of the matrix. These results would indicate a decrease in $R_{G,m}$ by up to 50% with increasing temperature for the big and broad fractions. $R_{G,m}$ was not measured, but it is unlikely to change significantly due to the extended nature of the PHIC in solution. The solvent quality should increase at least marginally with temperature. There would have to be an enormous change in the persistence length, though, in order to have an appreciable effect on the radius of gyration. A reduction in the persistence length by a factor of 2, which would be quite large, would only reduce the radius of gyration by 10–20%. Thus, any change in α caused by $R_{G,m}$ should be rather small.

Several difficulties must be mentioned in this discussion. One problem is that the stretched exponential fits were not always of high quality. In some instances the fits appeared to have systematic deviations from the data. Differences in the fit were observed if the value of D_0 was fit as a parameter instead of using the measured value of D_0, which has also been seen by Wheeler and Lodge.[2] They bring up the further concern that the stretched exponential is very sensitive to changes in α or u. Thus differences between experimental works from several sources cannot be reconciled by considering experimental error. They conclude that this must be due to inadequacies in the theory. The results here seem to lead to the same conclusion—that in its present form the hydrodynamic scaling theory does not provide an adequate description.

Comparison of Different Fractions vs Concentration/Temperature. Despite the lack of agreement with established theoretical models, a comparison between the different fractions may be made by examining the dependence of the translational diffusion coefficient of the polystyrene on the size of the polyisocyanate chain. The toluene results can be included in the comparison by using a reduced diffusion coefficient, D/D_0. The most obvious method is to compare the diffusion coefficient to the mass concentration of the PHIC. This is shown in Figure 6a. The sharpest decline in D/D_0 is seen for the big fraction. The broad fraction also shows a stronger concentration dependence in toluene than in tetrachloroethane. This is expected if the PHIC is more rigid in the toluene.

Several other ways may be used to observe the concentration dependence of the PS diffusion coefficient. If an assumption of complete rigidity of the PHIC is made, a length can be determined from either the Broersma or T–G theories. The dependence on the reduced concentration CL^3 can then be examined. The results are shown in Figure 6b for the Broersma rigid rod (they are qualitatively the same T–G). The toluene and TCE results disagree, because the rigid-rod assumption removes any effect of increasing rigidity in the toluene. The big fraction shows a weaker dependence on CL^3 than the other

fractions. The length can also be taken as the contour length of a wormlike chain. The results for this (Figure 6c) are quite similar to the rod results, again showing poor agreement between the different fractions.

For a polydisperse dispersion, the dimensionless concentration, CL^3, may, as was discussed in section 3, be taken as $C_m L_z L_w/\sigma$. If the values of L_z and L_w are replaced with the end-to-end distances of a wormlike chain with those contour lengths, then significantly better agreement is seen (Figure 6d). The end-to-end distance of a wormlike chain is given by

$$\langle R^2 \rangle = 2PL - 2P^2(1 - e^{-L/P}) \qquad (14)$$

where L is the contour length and P is the persistence length.[75] The toluene and TCE data agree, because the change in persistence length is taken into account ($P \sim 40$ nm in toluene, $P \sim 20$ nm in tetrachloroethane). This explains the sharper concentration dependence seen in toluene. The big and small fractions also show closer agreement, because the greater flexibility of the big fraction is accounted for.

A similar comparison may be made of the concentration dependence of the translational diffusion coefficient at different temperatures. The effect of temperature is not seen to be very great. Obviously the absolute value of the diffusion coefficient increases with increasing temperature. The reduced diffusion coefficient shows only a weak dependence on temperature. If one assumes complete rigidity, then there should not be an effect due to temperature. By the same method as above, the end-to-end distance of a wormlike chain may be used to compare data from different temperatures. The higher temperature diffusion coefficients show a slightly weaker dependence on concentration than the low temperature values. This is consistent with a decreasing persistence length with increasing temperature, which has been previously observed.[76] The change seen here is small, however, and is often difficult to separate from experimental error. The dependences seen indicate that the persistence length may decrease to ~15 nm at elevated temperature. The results are shown for the different fractions in Figure 7.

5. Fast Relaxation in Ternary Solutions

A second feature of the DLS spectra in some of the ternary solutions is a fast relaxational mode that is not present either in the binary solutions or in the ternary solutions with low PHIC concentrations. The appearance of a second relaxational mode in addition to the PS translational diffusion mode is of interest, since it may signal the onset of qualitatively different dynamical behavior and may therefore be an indication of the start of "semidilute behavior". The main reason for selecting an isorefractive ternary system was to avoid scattering from the matrix polymer, which can complicate the DLS spectra. The selection of a 390 000 M_m polystyrene was in part to avoid a probe that was large enough to exhibit internal chain motions in the DLS spectrum. The results from the binary solutions of PHIC/TCE and PS/TCE would suggest that unimodal behavior should be seen in the DLS spectra of the ternary solutions. Fast relaxations in DLS spectra in ternary isorefractive systems have been observed by a number of authors,[9,12-15,77-80] but a complete explanation of their origin is still lacking. The rates of the fast relaxation were characterized as functions of matrix size and concentration, scattering angle, and temperature.

Fast Relaxational Modes in Ternary Solution. The fast relaxational mode varies in intensity from zero to 5%, and this much smaller intensity than the PS translational diffusion made precise measurements of the relaxation

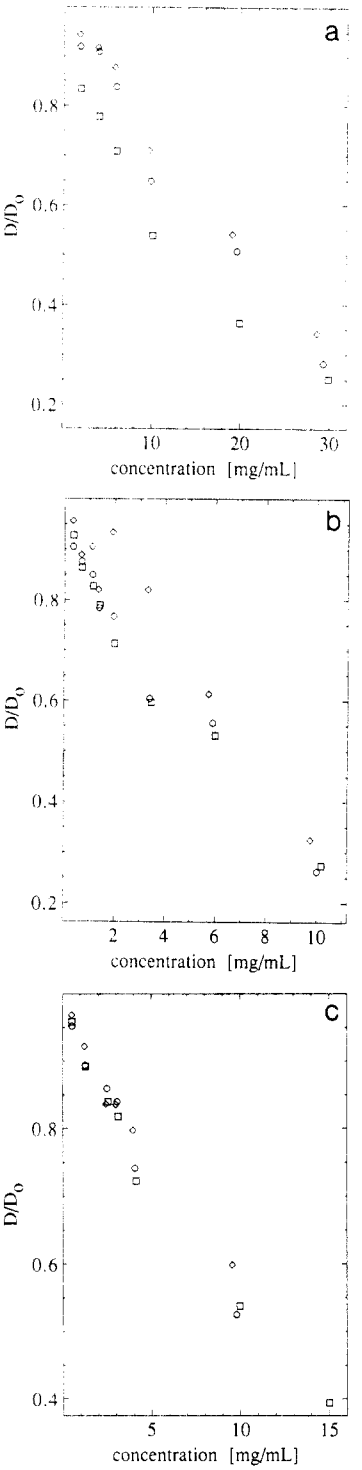

Figure 7. Reduced translational diffusion coefficient, D/D_0, of the polystyrene coil as a function of the concentration of PHIC in the ternary solution. a is for the broad fraction, b for the big fraction, and c for the small fraction. These are plotted for three different temperatures: (□) 25.0 °C; (○) 50.0 °C; (◇) 75.0 °C.

times difficult. For the lowest concentrations of PHIC the DLS spectra are unimodal, while at the highest concentrations the spectra are clearly bimodal. Two sample distributions determined with CONTIN are shown in Figure 8. Figure 8a is from a binary PS solution, and b is from a ternary solution with a fast relaxation mode. The binary PS solution measurement was obtained at high q. As discussed in I, the fast mode seen in this spectrum is most likely an artifact. The error in both amplitude and relaxation time is over 100%, and the translational diffusion mode fit is unchanged if this fast mode is suppressed. If the limits of integration are expanded, then this peak moves so that it is always at the edge of the range which was selected. In contrast, the ternary solution is

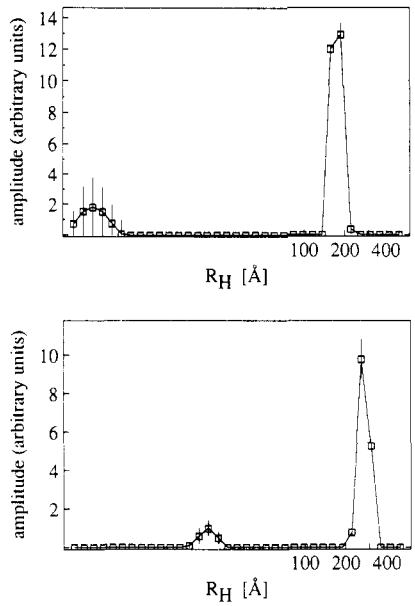

Figure 8. CONTIN analyses of representative correlation functions. a is for a 1.0 mg/mL PS solution in TCE, and b is for a 10.3 mg/mL broad PHIC/1.0 mg/mL PS solution in TCE. Both correlation functions were taken at $\Theta = 61.1°$ and $T = 25.0$ °C. The squares are the results obtained from CONTIN, and the line simply connects these points for ease of interpretation.

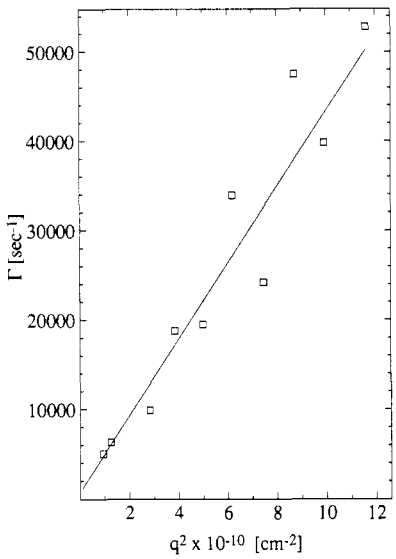

Figure 9. Relaxation constant, Γ, for the fast relaxation mode as a function of q^2. The sample was 1.0 mg/mL PS and 10.3 mg/mL broad PHIC in TCE at 25.0 °C. The slope of the linear fit is a diffusion coefficient that characterizes the fast motion.

unaffected by expanding the limits of integration. The fast peak shown for the ternary solution here is ~2% of the total amplitude, and the fast peak in the binary sample is only ~0.2%, although it may appear larger due to the logarithmic scale.

The relaxation frequency of the fast motion, Γ, exhibits a linear dependence on q^2, which is characteristic of diffusive motion. Apparent diffusion coefficients were determined from the slope of the linear fit in the Γ vs q^2 plot (see Figure 9) and are shown in Table 9. The apparent diffusion coefficient for the last relaxation, D_{fast}, is approximately 10 times larger than the PS translational diffusion coefficient, D_{slow}, in all of the ternary solutions in TCE (Table 10). In toluene, D_{fast} is approximately 4 times as large as D_{slow} (Table 11). The amplitude of the fast motion increases with increasing PHIC concentration. The amplitude also shows a small increase with increasing scattering vector, q.

Table 9. Diffusion Coefficients [$\times 10^7$ (cm²/s)] for Fast Relaxations in Ternary Solutions of PS/PHIC/TCE

conc (mg/mL)	25 °C	50 °C	75 °C
	Broad		
4.04	6.3 ± 6.1		
6.02	6.9 ± 1.1		
10.08	4.5 ± 0.5	6.4 ± 1.9	11.2 ± 4.7
19.98	2.9 ± 0.4	5.8 ± 1.2	14.1 ± 1.7
29.96	2.2 ± 0.2	5.8 ± 1.8	6.5 ± 1.8
	Big		
0.70	5.8 ± 2.4	6.9 ± 5.5	20.4 ± 8.0
1.14	7.0 ± 1.1	12.7 ± 5.0	22.8 ± 10.0
1.41	6.9 ± 5.1	9.5 ± 0.2	16.9 ± 4.3
2.00	7.9 ± 1.5	11.4 ± 5.1	15.0 ± 5.2
3.46	5.4 ± 0.8	8.1 ± 1.2	20.4 ± 2.4
6.00	4.8 ± 1.6	6.2 ± 1.0	19.6 ± 6.2
10.20	2.7 ± 0.4	2.3 ± 0.2	7.9 ± 1.8
	Small		
4.14	7.5 ± 5.3	8.2 ± 8.3	7.7 ± 13.0
8.38	5.9 ± 2.6	6.6 ± 1.4	12.3 ± 2.3
9.98	6.9 ± 2.3	10.4 ± 3.1	7.6 ± 1.3
15.02	3.0 ± 0.5		

Table 10. Ratio of Diffusion Coefficients for PS/PHIC/TCE Fast Relaxation/Slow Relaxation

conc (mg/mL)	25 °C	50 °C	75 °C
	Broad		
4.04	9.7 ± 9.5		
6.02	11.5 ± 1.9		
10.08	9.9 ± 1.1	7.5 ± 2.3	8.3 ± 3.5
19.98	9.6 ± 1.2	8.8 ± 1.8	13.8 ± 1.6
29.96	10.3 ± 1.1	15.6 ± 4.9	10.1 ± 2.7
	Big		
0.70	8.0 ± 3.3	6.0 ± 4.8	12.2 ± 4.8
1.14	10.2 ± 1.6	11.4 ± 4.5	13.3 ± 5.8
1.41	10.6 ± 7.9	9.3 ± 0.2	10.9 ± 2.8
2.00	13.3 ± 2.5	11.4 ± 5.1	8.5 ± 3.0
3.46	11.0 ± 1.5	10.2 ± 1.5	13.2 ± 1.6
6.00	10.9 ± 3.6	8.5 ± 1.4	16.9 ± 5.4
10.20	11.8 ± 1.8	6.8 ± 0.5	12.9 ± 3.0
	Small		
4.14	12.5 ± 8.8	11.9 ± 12.1	5.1 ± 8.6
8.38	12.9 ± 5.7	8.1 ± 1.8	9.4 ± 1.7
9.98	15.6 ● 5.3	15.1 ± 4.5	6.8 ± 1.1
15.02	9.2 ± 1.6		

Table 11. Polystyrene, MW = 390 K, in Ternary Solution: Broad PHIC/Toluene

conc of PHIC (mg/mL)	$D_{slow} \times 10^7$ (cm²/s)	$D_{fast} \times 10^7$ (cm²/s)	D_{slow}/D_{fast}
1.02	2.41 ± 0.09		
1.81	2.18 ± 0.08		
3.01	1.93 ± 0.04		
3.97	1.77 ± 0.08	6.50 ± 4.30	3.67 ± 2.44
5.01	1.58 ± 0.09	10.77 ± 7.20	6.82 ± 4.57
6.03	1.36 ± 0.10	5.70 ± 1.14	4.19 ± 0.89
7.02	1.38 ± 0.03	5.77 ± 1.31	4.18 ± 0.95
9.02	1.17 ± 0.04	4.56 ± 0.41	3.90 ± 0.37
10.20	0.92 ± 0.02	4.26 ± 1.07	4.64 ± 1.17
14.99	0.67 ± 0.03	2.11 ± 0.53	3.14 ± 0.80

Onset Concentration. It is widely accepted that there is no critical concentration separating dilute from semidilute solutions (i.e., in the sense of a phase transition). Rather, there is a gradually larger entanglement effect leading to a gradual crossover between the two regimes.[35,73] With increasing PHIC concentration the fast mode could be detected with greater precision, because of its increasing amplitude. The amplitude was small, however, at the lowest concentrations where it was observed, which made determination of an onset concentration difficult (in this section discussion of concentration effects always refer to PHIC concentration). It is probably the case that a fast mode exists at concentrations somewhat lower than can be detected in the DLS experiment.

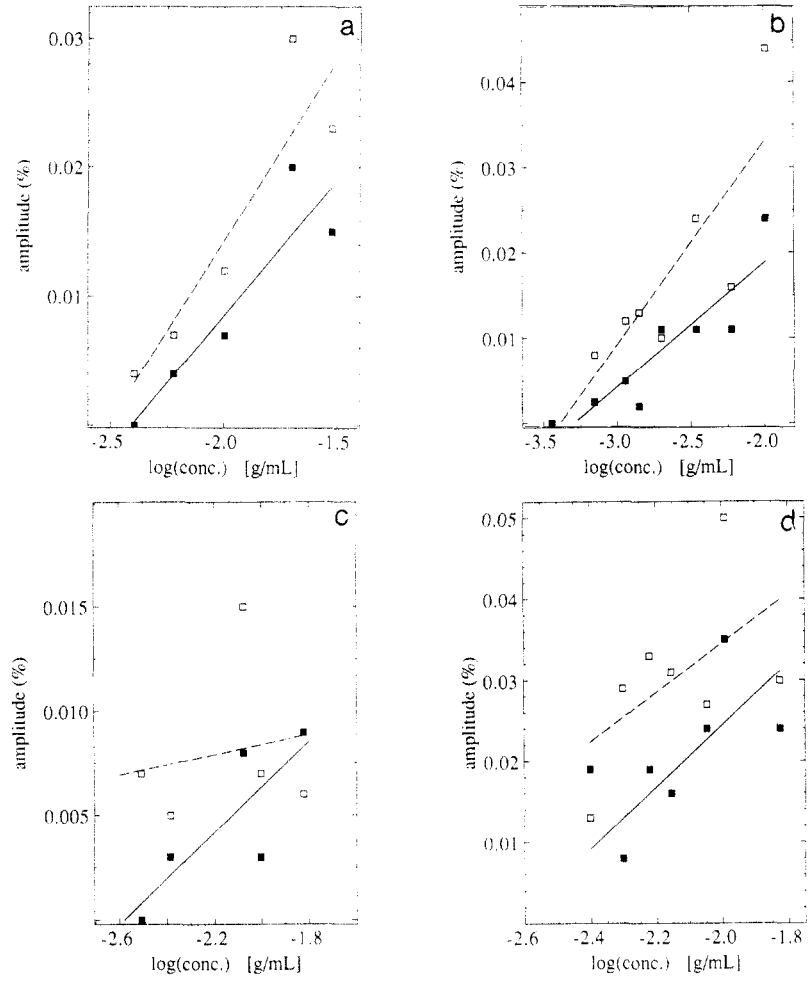

Figure 10. Amplitude of the fast relaxation as a function of concentration of PHIC in the ternary solution. Amplitude is given as a percentage of the total correlation function. The amplitude is given for both high scattering vectors (□) and low scattering vectors (■). The linear fits shown were used to extrapolate to zero amplitude to calculate an onset concentration for the fast mode. (- - -) Fit for high scattering vectors. (—) Fit for low scattering vectors. (a) Broad fraction of PHIC in TCE. (b) Big fractkion of PHIC in TCE. (c) Small fraction of PHIC in TCE. (d) Broad fraction of PHIC in toluene.

A fit of the amplitude of the fast mode vs concentration was used to extrapolate to zero amplitude in order to calculate an onset concentration for the fast mode, c_{fast}. Due to the error in the individual measurements, the amplitudes from several angles were combined as an average, and the fit was done using the amplitude for either a high or low scattering vector. Amplitudes for scattering angles >90° were used for the high scattering angle results, and amplitudes for angles <40° were used for the low scattering angle results.

A linear fit of amplitude vs concentration does not give meaningful results (the x-intercept, or onset concentration, is negative for each fraction) whereas a linear fit of amplitude vs log(concentration) provides more reasonable results (shown in Figure 10). For low scattering vectors the calculated onset concentrations, c_{fast}, in TCE are 3.8, 0.50, and 2.6 mg/mL for the broad, big, and small fractions, respectively. For high scattering vectors c_{fast} is 3.1, 0.41, and 0.1 mg/mL for the broad, big, and small fractions, respectively. In toluene c_{fast} for the broad fraction is 2.3 mg/mL for low q and 0.8 mg/mL for high q. These results show good agreement for the big and broad fractions in TCE, indicating onset concentrations slightly lower than the least concentrated solutions exhibiting bimodal DLS spectra.

The results for the small and broad fraction in toluene are not as clear. For both these fractions the high q onset concentrations determined above are very low and several samples with higher concentration were seen to be unimodal. In both fractions the ~4 mg/mL solutions show a very weak fast mode and the ~3 mg/mL solutions are unimodal. The onset concentrations of 2.6 and 2.3 mg/mL for small and broad/toluene, respectively, could be an indication that the amplitude of the fast relaxation is nonzero but too small to measure in the 3 mg/mL solutions. Since there is no critical concentration where a fast mode suddenly appears, then there is probably a small concentration range where a fast mode exists but is too weak to detect.

The determination of a reduced onset concentration (in terms of CL^3) to compare to D–E theory is complicated by two factors. First, it is clear from the discussion above that a range of mass concentrations should be considered (instead of a single exact value). The lower limit of this range is taken as the onset concentration of the fast mode calculated using low scattering vector data. The upper limit is taken as the lowest concentration at which bimodal behavior is experimentally observed.

The second complicating factor is the determination of the size and shape of the PHIC. This has been discussed in sections 2 and 3, where analysis of either the PHIC diffusion in dilute solution or the PS diffusion in ternary solution leads to the conclusion that PHIC is a wormlike chain (i.e., not a rigid rod). As in section 3, when comparing the PS translational diffusion through different fractions of PHIC, there are several different ways to determine a reduced concentration. The simplest way is to assume the PHIC is perfectly rigid and use an apparent length calculated from the diffusion coefficient found by DLS in chloroform. All of the fractions show similar onset

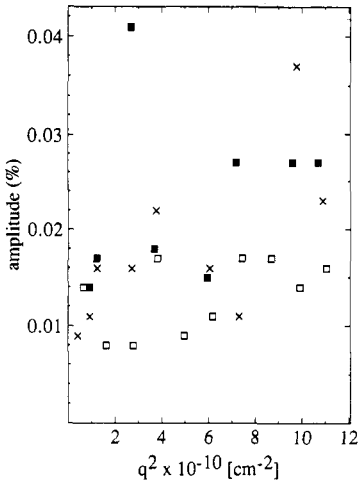

Figure 11. Amplitude of the fast relaxation as a function of scattering vector. The amplitude is given as a percentage of the total correlation function. The sample was a ternary solution with 6.0 mg/mL big PHIC in TCE. The results are given for three different temperatures: (□) 25.0 °C; (×) 50.0 °C; (■) 75.0 °C.

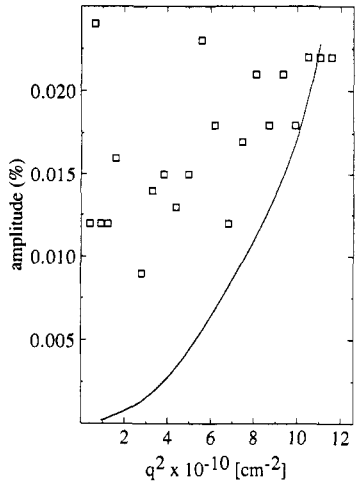

Figure 12. Amplitude of the fast relaxation as a function of scattering vector. The amplitude is given as a percentage of the total correlation function. The sample was a ternary solution with 20.0 mg/mL broad PHIC in TCE at 25.0 °C. (□) The experimental data. The results are compared to a theoretical prediction for the first internal mode of a 390 000 MW polystyrene coil (—).

concentrations when analyzed this way, with $CL^3 \sim 5$–10. Another method is to use the contour length of the wormlike chain as the length, L, which gives $CL^3 \sim 7$–15 for the onset concentration. The range of onset concentration of the fast mode for each fraction is large enough that all of the fractions give consistent onset values regardless of how L is selected. The broad fraction in toluene appears to have a somewhat smaller onset concentration than the broad fraction in TCE, but this difference is inconclusive since it is smaller than the experimental error.

Fast Mode Discussion. Several explanations for the presence of a fast mode that do not rely on special dynamical features are discussed below. These, however, do not appear adequate to describe the observed dynamical behavior, so additional explanations have been proposed to provide a physical basis for the dynamic behavior.

The possibility of incomplete index matching is effectively ruled out by the temperature dependence of this mode. At 75 °C the PHIC is completely index matched in tetrachloroethane (within ±0.001 mL/g, the experimental error). At 25 °C the value of the differential index of refraction is at least 10 times larger (although still more than 10 times smaller than for PS). The experimental results indicate no significant difference in the amplitude of the fast relaxation with changing temperature (shown for a representative sample at 25, 50, and 75 °C in Figure 11). The temperature dependence was also measured in toluene for one fraction with a PHIC concentration of 10.3 mg/mL. The fast mode amplitude is constant, despite the difference in degree of index matching. Thus, as expected, the amount of light scattered from the rods is not sufficient to be observed in this experiment.

Another consideration is the slowest internal DLS mode of polystyrene, which might possibly be observed at the scattering vectors used for a 390 000 molecular weight chain (see I). The fast mode observed here does not have a nonzero intercept or a slope equal to the translational diffusion coefficient of the coil (see Figure 9), both of which are expected from the prediction for the first internal mode of a Gaussian coil (relaxation frequency, $\Gamma = q^2D + 2/\tau_1$). The increase in amplitude with increasing q is also much weaker than that calculated for the first internal mode (Figure 12) of either a free-draining flexible coil[81] or a nondraining or partly draining flexible coil.[82,83] In addition, the relaxation times measured are also larger than predicted for the first internal mode.

The possibility of bimodal behavior in the correlation spectrum from homogeneous mixtures of two flexible polymers in a solvent where one of the polymers is isorefractive has been raised by Benmouna et al.[44] The predictions of this theory have been observed experimentally,[78–80] but in order to best see the bimodal behavior, concentrations of the "visible" polymer were as high as 80% of the total polymer fraction. The general idea behind this theory is that the coupling of the concentration fluctuations of the two different polymers contributes to the light scattering, even though concentration fluctuations in the isorefractive polymer with respect to itself do not cause scattered light. This is in addition to the light scattered by concentration fluctuations in the visible polymer with respect to itself.

Discrepancies exist between the experimental measurements here and the dependences on polymer concentration predicted by the Benmouna theory. The major trend predicted by Benmouna is an increase in bimodal behavior with an increase in the relative amount of nonisorefractive (or visible) polymer. In this study the relative amount of visible polymer decreases as the PHIC concentration increases (because the PS concentration remains fixed). The amount of bimodal behavior measured increases and is a maximum for the smallest fraction of visible polymer. A slight increase in bimodal behavior with an increase in total polymer fraction is also predicted, but this is a much weaker dependence than that from the decreasing polymer fraction. Thus it is not enough to offset the decrease associated with the smaller fraction of visible polymer present when the total polymer concentration is high.

Obviously, the background polymer in this investigation, PHIC, is not a flexible polymer, but one might expect certain qualitative predictions to hold true. In the limit of zero concentration of visible polymer, however, the Benmouna theory predictions reduce to a single relaxation. In this case it appears that the PS is present in dilute enough amounts to expect the single exponential prediction from the Benmouna theory.

Foley and Cohen[84] have developed a theory to describe both concentration fluctuations and spinodal decomposition in systems with two polymers and a solvent. They also predict bimodal behavior in the DLS spectra, but their analysis only considers long time scales of

$$t \gg R_G^2/D_s \qquad (15)$$

where R_G^2 and D_s are the radii of gyration and self-diffusion coefficient for either species. This allows them to disregard coupling of inter- and intramolecular dynamics; however, the fast relaxations measured here occur at a time shorter than the time t above, so this theory cannot provide a valid description of these fast motions.

Other Possibilities. Another possible explanation for the presence of a fast mode is non-Fickian diffusion.[11] This entails the probe undergoing fast diffusion over short distances where it might not be fully affected by the matrix, while the overall diffusion in solution is slower. At low q the fast, short-range motions contribute weakly to the decay. Both short- and long-range motion should be observed as q increases,[11] which would agree with the amplitude dependence on q observed here. The fast mode relaxation rate exceeds the binary probe diffusivity, however, and it seems unlikely that the local solution structure could be such that the probe would undergo short-range diffusion that was faster than seen in pure solvent. This leads to the conclusion that non-Fickian diffusion is unlikely to cause the fast mode.

Chu and Wu[77] have suggested that matrix coupling can cause deviations from single exponential DLS spectra. Presumably the PS will be affected by the motions of the PHIC matrix. If these are of different frequency than the PS translational diffusion, then a second mode will be observed in the DLS spectra. In dilute solution the PHIC translates more quickly than PS does, so an additional mode caused by this coupling would be expected to be a fast mode. The presence of this mode should depend most strongly on the total mass of the matrix polymer present, since this will increase the number of interactions. As the matrix size increases the fast relaxation would be expected to slow, since the matrix motions (which cause the coupling) would slow. The fast amplitude here is seen to depend strongly on the matrix size when samples with equal mass concentration are considered. Thus a simple coupling of the PS chain to the motion of individual PHIC chains does not seem to be occurring.

Another possible coupling to the matrix would be between the PS and groups of the PHIC chains. At the concentrations where the fast mode appears the PS is surrounded by many matrix chains. If these matrix chains remained fixed, then the PS would be severely constrained and would almost certainly have to translate by reptation. The translational diffusion coefficient results for the PS chain show that reptation does not occur. It is possible, however, that on a short time scale the PS chain is constrained or "caged" by neighboring PHIC chains. The idea of caging is well-known and has been used to predict the rotational diffusion of rodlike polymers in semidilute solution.[17-19,34,85]

In the complex solutions studied here, the coil could be hindered in its motion at some given instant and would remain hindered for the time it took the surrounding rods to diffuse a short distance, thus allowing the coil to freely move. The rate of the fast relaxation would be dependent on the rate of the release mechanism, which would depend on the rate of diffusion of the rods through some fraction of their length. The amount of caging that lasts long enough to hinder the PS coil translations should increase as the matrix size and concentration increases. The relaxation rate of the cages would also be expected to increase with increasing matrix size and concentration. The overall translational motion would not be strongly affected, because the polystyrene would only be hindered for very short times. These predictions are in general agreement with the experimental results seen here.

Although it is not clear that this is the correct explanation, it is certain (as has been mentioned elsewhere[11]) that the presence of an additional mode in the DLS spectra needs to be properly handled in the data analysis so as not to bias the translational diffusion results. The presence of a second relaxation in the DLS spectra does seem indicative of semidilute behavior. Using this criterion, a precise measure of the onset of the semidilute regime is elusive because of the low precision in the data and the likely gradual onset of the semidilute regime. Thus an attempt to fix a precise number where entanglements become important is probably futile. It can be seen, however, that the fast relaxation appears for $CL^3 \sim 5$–15 (if the PHIC length is determined assuming it to be a rigid rod), and this onset concentration agrees with those found from measuring rotational diffusion in rod systems.[23,30,34]

6. Conclusion

This work has attempted to provide further insight into semidilute solutions of semirigid polymers. It was shown that an isorefractive system could be designed where a semirigid polymer was the matrix chain. Very few studies of this type have been attempted. The probe particle was a linear polystyrene, and to our knowledge this is the first study to observe dynamics of such a semidilute mixture.

Perhaps the most important observation here is that chain flexibility in the semirigid polymer must be considered. Poly(*n*-alkyl isocyanates) have often been treated as rigid rods for the purpose of theoretical simplicity, but analysis of both the dilute and semidilute solutions of PHIC (binary and ternary solutions, respectively) assuming rigid-rod behavior was found to be inadequate. The different fractions of PHIC had equivalent "entangling power" if a reduced concentration of $CL\langle R^2\rangle$ was used (where $\langle R^2\rangle$ was the end-to-end distance of the wormlike chain), which was demonstrated through the dependence of the translational diffusion coefficient of the PS probe on the PHIC concentration.

The onset of semidilute behavior was inferred from the occurrence of a fast mode in the DLS spectra (in addition to the PS translational diffusion mode). This fast mode had a low intensity at the onset concentration and grew in intensity with increasing PHIC concentration, although it was always a small amount of the total spectrum ($\sim$5% or less). It was necessary to fit this mode, however, to avoid biasing the translational diffusion results. A rough approximation of the onset of the semidilute regime was found to be $CL^3 \sim 5$–15.

A number of simple explanations were seen to be inadequate to describe this fast mode behavior. Therefore, it was necessary to consider special dynamical behavior, which led to the inference that this mode signaled the onset of semidilute behavior. The most likely explanation is that some sort of coupled motion between the probe and matrix causes the bimodal DLS spectra. An overall description of the dynamics in the ternary solution that emerges from these experiments is as follows, although it should be stressed that this description is still tentative. On a sufficiently long length and time scale the PS chains move through solution pushing PHIC chains out of their way. Although relatively small deviations from Stokes–Einstein behavior are seen, the probe essentially moves as if the PHIC/solvent mixture acted as a viscous solvent. On a short length and time scale the motion of the PS differs from how it would behave in a solvent of small molecules, as it is affected by the local solution structure. This short time behavior could be due to transient caging of the PS chain by the PHIC matrix. Further studies of systems of this type seem warranted to better understand the non-single-exponential behavior of the DLS spectra, since information about the detailed dynamic behavior of the solution is most probably contained therein.

Acknowledgment. This work was supported by National Science Foundation Grant CHE-9119676 (to R.P.) and by the NSF–MRL program through the Center for Materials Research at Stanford University.

References and Notes

(1) Cantor, A. S.; Pecora, R. *Macromolecules*, previous paper in this issue.
(2) Wheeler, L. M.; Lodge, T. P. *Macromolecules* **1989**, *22*, 3399.
(3) Hanley, B.; Balloge, S.; Tirrell, M. *Chem. Eng. Commun.* **1983**, *24*, 93.
(4) Martin, J. E. *Macromolecules* **1986**, *19*, 922.
(5) Cotts, D. B. *J. Polym. Sci., Polym. Phys. Ed.* **1983**, *21*, 1381.
(6) Numasawa, N.; Kuwamoto, K.; Nose, T. *Macromolecules* **1986**, *19*, 2593.
(7) Hadgraft, J.; Hyde, A. J.; Richards, R. W. *J. Chem. Soc., Faraday Trans. 2* **1979**, *75*, 1495.
(8) Pu, Z.; Brown, W. *Macromolecules* **1989**, *22*, 890.
(9) Phillies, G. D. J.; Ullmann, G. S.; Ullmann, K.; Lin, T.-H. *J. Chem. Phys.* **1985**, *82*, 5242.
(10) Brown, W.; Rymdén, R. *Macromolecules* **1988**, *21*, 840.
(11) Mustafa, M.; Russo, P. S. *J. Colloid Interface Sci.* **1989**, *129*, 240.
(12) Brown, W.; Rymdén, R. *Macromolecules* **1986**, *19*, 2942.
(13) Yang, T.; Jamieson, A. M. *J. Colloid Interface Sci.* **1988**, *126*, 220.
(14) Jamieson, A. M.; Southwick, J. G.; Blackwell, J. *J. Polym. Sci., Polym. Phys. Ed.* **1982**, *20*, 1513.
(15) Russo, P. S.; Mustafa, M.; Cao, T.; Stephens, L. K. *J. Colloid Interface Sci.* **1988**, *122*, 120.
(16) Tracy, M. A.; Pecora, R. *Macromolecules* **1992**, *25*, 337. Tracy, M. A.; Garcia, J.-L.; Pecora, R. *Macromolecules* **1993**, *26*, 1862.
(17) Jamil, T.; Russo, P. S.; Negulescu, I.; Daly, W. H.; Schaefer, D. W.; Beaucage, G. *Macromolecules* **1994**, *27*, 171.
(18) Doi, M. *J. Phys. Fr.* **1975**, *36*, 607. Doi, M.; Edwards, S. F. *J. Chem. Soc., Faraday Trans. 2* **1978**, *74*, 560.
(19) Doi, M.; Edwards, S. F. *The Theory of Polymer Dynamics*; Clarendon Press: Oxford, 1986.
(20) Maguire, J. F. *J. Chem. Soc., Faraday Trans. 2* **1981**, *77*, 513.
(21) Jain, S.; Cohen, C. *Macromolecules* **1981**, *14*, 759.
(22) Mori, Y.; Ookubo, N.; Hayakawa, R.; Wada, Y. *J. Polym. Sci., Polym. Phys. Ed.* **1982**, *20*, 2111.
(23) Zero, K. M.; Pecora, R. *Macromolecules* **1982**, *15*, 87.
(24) Kubota, K.; Chu, B. *Biopolymers* **1983**, *22*, 1461.
(25) Kubota, K.; Chu, B. *Macromolecules* **1983**, *16*, 105.
(26) Statman, D.; Chu, B. *Macromolecules* **1984**, *17*, 1537.
(27) Russo, P. S.; Karasz, F. E.; Langley, K. H. *J. Chem. Phys.* **1984**, *80*, 5312. DeLong, L. M.; Russo, P. S. *Macromolecules* **1991**, *24*, 6139. Jamil, T.; Russo, P. S. *J. Chem. Phys.* **1992**, *97*, 2777.
(28) Keep, G. T.; Pecora, R. *Macromolecules* **1985**, *18*, 1167.
(29) Keep, G. T. Ph.D. Thesis, Stanford University, Stanford CA, 1986.
(30) Keep, G. T.; Pecora, R. *Macromolecules* **1988**, *21*, 817.
(31) Doi, M.; Shimado, T.; Okano, K. *J. Chem. Phys.* **1988**, *88*, 4070.
(32) Maeda, T. *Macromolecules* **1989**, *22*, 1881.
(33) Maeda, T. *Macromolecules* **1990**, *23*, 1464.
(34) Teraoka, I.; Ookubo, N.; Hayakawa, R. *Phys. Rev. Lett.* **1985**, *55*, 2712.
(35) Teraoka, I.; Hayakawa, R. *J. Chem. Phys.* **1989**, *91*, 7951.
(36) Fixman, M. *Phys. Rev. Lett.* **1985**, *54*, 337.
(37) Berry, G. C.; Cotts, P. M.; Chu, S.-G. *Br. Polym. J.* **1981**, *13*, 47.
(38) Ying, Q.; Chu, B.; Qian, R.; Bao, J.; Zhang, J.; Xu, C. *Polymer* **1985**, *26*, 1401.
(39) Aharoni, S. M. *Macromolecules* **1979**, *12*, 537.
(40) Aharoni, S. M. *Polymer* **1980**, *21*, 21.
(41) Lewis, R. J. Ph.D. Thesis, Stanford University, Stanford, CA, 1985.
(42) Cantor, A. S. Ph.D. Thesis, Stanford University, Stanford, CA, 1991.
(43) Kaddour, L. O.; Strazielle, C. *Polymer* **1987**, *28*, 459.
(44) Benmouna, M.; Benoit, H.; Duval, M.; Akcasu, Z. *Macromolecules* **1987**, *20*, 1107.
(45) Aharoni, S. M. *Macromolecules* **1979**, *12*, 94.
(46) Shashoua, V. E.; Sweeny, W.; Tietz, R. F. *J. Am. Chem. Soc.* **1960**, *82*, 866.
(47) Bur, A. J.; Fetters, L. J. *Chem. Rev.* **1976**, *76*, 727.
(48) Tonelli, A. E. *Macromolecules* **1974**, *7*, 628.
(49) Mansfield, M. L. *Macromolecules* **1986**, *19*, 854.
(50) Cook, R. *Macromolecules* **1987**, *20*, 1961.
(51) Cook, R.; Johnson, R. D.; Wade, C. G.; O'Leary, D. J.; Muñoz, B.; Green, M. M. *Macromolecules* **1990**, *23*, 3454.
(52) Broersma, S. *J. Chem. Phys.* **1960**, *32*, 1626.
(53) Broersma, S. *J. Chem. Phys.* **1960**, *32*, 1632.
(54) Broersma, S. *J. Chem. Phys.* **1981**, *74*, 6989.
(55) Newman, J.; Swinney, H. L.; Day, L. A. *J. Mol. Biol.* **1977**, *116*, 593.
(56) Kuwata, M.; Murakami, H.; Norisuye, T.; Fujita, H. *Macromolecules* **1984**, *17*, 2731.
(57) Rubingh, D.; Yu, H. *Macromolecules* **1976**, *9*, 681.
(58) Murakami, H.; Norisuye, T.; Fujita, H. *Macromolecules* **1980**, *13*, 345.
(59) Tirado, M. M.; García de la Torre, J. *J. Chem. Phys.* **1979**, *71*, 2581.
(60) Tirado, M. M.; Martínez, C. L.; García de la Torre, J. *J. Chem. Phys.* **1984**, *81*, 2047.
(61) Yamakawa, H.; Fujii, M. *Macromolecules* **1973**, *6*, 407.
(62) Reference 61 reprinted in: *Polymer Solution Properties Part II: Hydrodynamics and Light Scattering*; Hermans, J. J., Ed.; Dowden, Hutchinson and Ross, Inc.: Stroudsburg, PA, 1978. This includes the correct form of eq 49 from the original paper.
(63) Berger, M. N.; Tidswell, B. M. *J. Polym. Sci. (Part C), Symp.* **1973**, *42*, 1063.
(64) Schneider, N. S.; Furusaki, S.; Lenz, R. W. *J. Polym. Sci., Part A-3* **1965**, 933.
(65) Yamakawa, H.; Fujii, M. *Macromolecules* **1974**, *7*, 128.
(66) Mori, Y.; Ookubo, N.; Hayakawa, R.; Wada, Y. *J. Polym. Sci., Polym. Phys. Ed.* **1982**, *20*, 2111.
(67) Gupta, A. K.; Benoit, H.; Marchal, E. *Eur. Polym. J.* **1979**, *15*, 285.
(68) Chang, T.; Han, C. C.; Wheeler, L. M.; Lodge, T. P. *Macromolecules* **1988**, *21*, 1870.
(69) Kent, M. S.; Tirrell, M.; Lodge, T. P. *Polymer* **1991**, *32*, 314 and references therein.
(70) Brown, W.; Zhou, P. *Macromolecules* **1989**, *22*, 4031.
(71) Ullmann, G. S.; Ullmann, K.; Lindner, R. M.; Phillies, G. D. J. *J. Phys. Chem.* **1985**, *89*, 692.
(72) Phillies, G. D. J.; Ullmann, G. S.; Ullmann, K.; Lin, T.-H. *J. Chem. Phys.* **1985**, *82*, 5242.
(73) de Gennes, P.-G. *Scaling Concepts in Polymer Physics*; Cornell University Press: London, 1979.
(74) de Gennes, P.-G. *J. Chem. Phys.* **1971**, *55*, 572.
(75) Yamakawa, H. *Modern Theory of Polymer Solutions*; Harper and Row: New York, 1971.
(76) Bianchi, E.; Ciferri, A.; Conio, G.; Krigbaum, W. R. *Polymer* **1987**, *28*, 813.
(77) Chu, B.; Wu, D.-Q. *Macromolecules* **1987**, *20*, 1606.
(78) Borsali, R.; Duval, M.; Benmouna, M. *Polymer* **1989**, *30*, 610.
(79) Borsali, R.; Duval, M.; Benmouna, M. *Macromolecules* **1989**, *22*, 816.
(80) Brown, W.; Konák, C.; Johnsen, R. M.; Zhou, P. *Macromolecules* **1990**, *23*, 901.
(81) Berne, B. J.; Pecora, R. *Dynamic Light Scattering*; Wiley-Interscience: New York, 1976.
(82) Perico, A.; Piaggio, P.; Cuniberti, C. *J. Chem. Phys.* **1975**, *62*, 2690.
(83) Nicolai, T.; Brown, W.; Johnsen, R. *Macromolecules* **1989**, *22*, 2795.
(84) Foley, G.; Cohen, C. *Macromolecules* **1987**, *20*, 1891.
(85) Odijk, T. *Macromolecules* **1983**, *16*, 1340.